ADSORPTIVE CHARACTERISTICS OF PHOSPHORUS ON FOUR BIOCHAR TYPES

BY

TETTEH, JOSEPH LAWER

(10397332)

THIS THESIS IS SUBMITTED TO THE UNIVERSITY OF GHANA, LEGON IN PARTIAL FULFILLMENT OF THE REQUIREMENT FOR THE AWARD OF M.PHIL SOIL SCIENCE DEGREE

JULY, 2014

DECLARATION

I hereby declare that this thesis, "adsorptive characteristics of phosphorus on four biochar types", has been written by me and that it is the true record of my own research work. It has neither in part been presented for another degree elsewhere. Works of other researchers have been duly cited by references to the authors and all assistance received also acknowledged.

TETTEH, JOSEPH LAWER

Dr. E. K. NARTEY

(PRINCICIPAL SUPERVISOR)

PROF. S. K. ADIKU

(SUPERVISOR)

ACKNOWLEDGEMENTS

I would also like to express my deepest gratitude to Dr. E. K. Nartey for his patience, guidance, comments, support, encouragement and securing funds to support the work. Godly richly bless you. Many thanks to Prof. S. K. Adiku, I cannot forget your contribution to the success of this research work.

I wish to say a big thank you to all Lecturers of the Department of Soil, University of Ghana, Legon for their advice during seminars that have helped to put this work together. I am particularly grateful to Dr. S. K. Asomaning for being there for any time I call on him.

My heartfelt thanks also go to the Globe Urban Food^{Plus} Project for providing financial assistance and the necessary laboratory logistics for the work. A very special thank you to Prof. Bernd Marschner of the Ruhr University, Bochum for agreeing to let me come and board the Globe Urban Food Plus Project. May the almighty God bless you.

My sincerest thanks go to all the Technical Staff of the Department of Soil Science Laboratory, Ecological Laboratory and Biotechnology Laboratory all of the University of Ghana, Legon. I say a big thank you Mr Julius Nartenor, Mr. Victor Edusei, and Mr. Daniel Darko for their support during my laboratory analysis.

Finally, I wish to thank Dr. Noah Adamtey and his wife for always reminding me to work very hard on my thesis to enable me submit on time.

DEDICATION

Dedicated to the glory of God, my parents and my wife. God bless you all.

TABLE OF CONTENT

LIST OF TABLES

LIST OF FIGURES

ABSTRACT

Biochar prepared from cocoa pod, sawdust, rice straw and husk wastes may provide new low cost technology for environmental management with emphasis on P removal from waste water to minimize eutrophication and to enhance P availability in tropical soils. To achieve this, the sorption characteristics of the biochar types would have to be understood. In this study, laboratory experiments were conducted to investigate the P adsorptive characteristics on four biochar types derived from cocoa pod, sawdust, rice husk and straw. Batch sorption experiment was conducted to investigate the time for maximum adsorption by shaking at two (2) hours intervals between 2 to 24 hours. X-ray diffractograms of the various biochars were obtained to help elucidate possible mechanisms of adsorption. Effect of pH on adsorption was also studied for initial pH ranging between 2 and 12 and initial P concentrations between 0.4 mM and 1.6 mM. Results from the research revealed that six (6) hours of shaking time was sufficient to achieve maximum adsorption onto the various biochars. Optimum pH for adsorption occurred at equilibrium pH of 5.7 for rice husk, 6.2 for sawdust, 6.7 for cocoa pod and 7.2 for the rice straw biochar. The isotherms indicated that the amount of P adsorbed increased with increasing equilibrium P concentrations. Increases in equilibrium pH above 7.2 led to decreases in adsorption for all the biochar types. Rice husk and sawdust biochar types were found to have the highest affinity for P with estimated maximum adsorption of 7300 mg/kg P. Phosphate adsorption mechanism varied with biochar type. Surface precipitation of P by Ca and Mg was proposed as an important mechanism of P adsorption on the sawdust biochar. Magnesium precipitation of P was also proposed as a mechanism of P removal by the rice husk biochar. Both electrostatic attraction and ligand exchange reactions by periclase (MgO) with P could be the main mechanisms of adsorption on cocoa pod, rice straw and sawdust

biochar types. Phosphorus adsorption via ligand exchange and or electrostatic attraction could have accounted for P removal by the rice husk biochar.

CHAPTER ONE

INTRODUCTION

1.0 Background

There are many different types of biomass resources in Ghana including agricultural crop residues, agricultural by-products, forestry residues, wood waste, and organic portion of municipal solid waste (Duku *et al.*, 2011). The major crop residues generated in the country include rice straw, rice husk, cocoa pods, stalk of maize, sorghum, millet and pineapple peels, etc. Ghana produces 13000 tonnes of waste daily; a bulk of which is organic, but the country lacks the appropriate infrastructure to manage the waste (Foray, 2012). Any technology that will transform these organic wastes into useful material will therefore be of immense benefit to the country.

There are mountains of sawdust in almost all districts of the country because of the activities of wood industries consisting of sawmills and carpentry workshops. These sawmills generate 20% of the total volume of wood milled as sawdust alone, excluding other wood waste (United Nations Industrial Development Organization [UNIDO], 2009). The mountains of sawdust are mainly disposed of through aerobic burning which culminates in the release of greenhouse gases (GHGs).

As a national policy to cut down on rice importation, there has been a conscious effort to boost rice production in Ghana. This has led to the generation of large volumes of rice straw and husk. Rice husk as an agricultural waste abounds in almost all rice-growing centres in Ghana and accounts for 23% of total paddy weight (Frimpong-Manso *et al.*, 2011). The high C: N ratio of rice husk makes the material not easily decomposable and thus unsuitable for use as soil amendment. Consequently, the material piles up breeding rodents such as mice that in turn attract snakes to the breeding sites. Rice straw is also a waste generated in the rice growing fields after harvesting.

Some of the rice straw are being used as feed for cattle and are occasionally incorporated into the soil during ploughing. The main method of disposal of these two materials has however, been through aerobic burning which also culminate in the release of GHGs.

Ghana is presently the world's second largest producer of cocoa beans. In the year 2012, Ghana produced over 1,000,000 metric tonnes of cocoa beans (USDA, 2012). However, the production of one tonne of marketable cocoa entails the harvest and breaking of approximately between 25,000 and 30,000 pods (Sustainable Tree Crop Production [STCP], 2007). These cocoa pods are dumped near farm steads on the plantations and become a significant source of disease inoculum when used as mulch on the plantations (Figueira, 1993). Some decades ago, the cocoa pods were ashed and used in the preparation of soap. However, with the influx of imported soap, the locally manufactured soap from cocoa pods is not so popular with Ghanaians leading to the piling up of the cocoa husk. Any technology that will transform the pods into a useful material will go a long way in reducing tonnage of waste produced from cocoa.

Pyrolysis can be a potential promising method of managing rice husk, rice straw, sawdust and cocoa pod compared to the current landfilling, incineration, or direct agricultural utilization, with their attendant secondary pollution problems (Lu *et al.*, 2011; Hwang *et al.*, 2007). The pyrolysis process tends to reduce the volume of bio-solids, eliminate pathogens and change the organic matter into bio-fuel, bio-oil and biochar (Lu *et al.*, 2011; Domi'guez *et al.*, 2006). Biochar pyrolysed from agricultural waste has large surface area and contain high elemental carbon and phosphorus, with a large amount of exchangeable cations. These positive attributes could be explored to improve soil fertility (Hossain *et al.*, 2010, 2011; Lu *et al.*, 2011).

Ghanaian soils are characterized by low organic carbon content and consequently low nitrogen contents. They are also highly weathered and dominated by oxides of Fe and Al with low P levels

(Nartey *et al.*, 1997). They also have large capacity to fix added P through sorption and anion exchange (FAO, 2011; Owusu-Bennoah *et al.*, 2000). Strongly sorbed or fixed phosphate in these soils are unavailable for plant uptake. Therefore, substantial P inputs are required for optimum plant growth (IAEA, 2002). Sorption of phosphorus fertilizers by aluminium and iron oxides, and highly weathered kaolinitic clays in these tropical soils results in decrease of plant available phosphorus (Owusu-Bennoah *et al.*, 2000). However, in most developing countries like Ghana, cost of fertilizers are high making it difficult for the poor farmers to apply large amounts of P to satisfy plant requirement (International Atomic Energy Agency [IAEA], 2002). Meanwhile, organic inputs that farmers can depend upon to minimise P fixation require frequent application because of high temperatures and rapid decomposition rates in the tropical environment. High haulage costs of organic residue from deposition points leading to high production cost is a big disincentive to many Ghanaian farmers for using these organic residues.

In northern Ghana where rainfall is uni-modal, organic additions especially from plant sources to soils are rare as the materials serve as feed for animals during the seven-month long dry season. Organic amendments to soils must therefore be in the form that will persist for very long periods to minimize frequent applications.

The world's resources of P are the smallest and thus on a global scale, P should be used as efficiently as possible in order to conserve the resource base and to maintain and increase where necessary, agricultural productivity (FAO, 2011). Any amendment or conditioner that when added to the soil will enhance P availability and persist in the soil will go a long way in making P sustainability a reality. This amendment must also have the additional property of being cheap and affordable to the resource poor Ghanaian farmer. A material that is inherently rich in P, stable in

the soil and can adsorb nutrients and release the nutrient slowly for plant use should be the panacea to the problem.

Biochar is a stable carbon rich material, which has gained a lot of attention for the numerous roles it plays in the soil. It is a product of biomass pyrolysis, which is the combustion in oxygen limited environment (Lehman *et al.*, 2006). It is highly resistant to microbial degradation and can therefore stay in soils for hundreds to thousands of years (Lehman *et al.*, 2006). It has been found to increase cation exchange capacity, soil pH, nutrient concentration and water retention of soils in addition to sequestering carbon from the atmosphere (Chen *et al.*, 2008; Lehmann, 2007; Tang *et al.*, 2013). It has been proven that biochar gradually releases limiting nutrients such as P (Uchimiya *et al.*, 2010). Research has shown that biochar has high ability to adsorb anions including P, cations and other non-polar organic compounds (Yao *et al.*, 2011; Kolodynska *et al.*, 2012).

1.1 Problem Statement

Although many studies have demonstrated the ability of biochar to sequester carbon and improve soil productivity, its use as an adsorbent in removing contaminants from wastewater is now gaining grounds. Biochar is a highly porous material containing functional groups such as the carboxylic and phenolic groups which influence its surface chemistry such as CEC and surface acidity. It also has large surface area that greatly influences its sorption properties (Tang *et al.*, 2013). In addition, it has high oxides and carbonate contents and high pH which vary with feedstock (Zheng *et al.*, 2013). These characteristics of biochar imply that the material has sorption properties that may vary with feedstock and pyrolysis temperature. According to Lehman (2007), biochar can adsorb more than 3000 mg/kg phosphates even at low solution concentrations of 40 mg/L whilst soil with low native P can adsorb only up to 600 mg/kg phosphates. This high adsorptive capacity of biochar implies that the material could be beneficial in removing P. The phosphate ladened biochar when

applied to soil could improve the P contents of tropical soils. Yao *et al.* (2011), studied the effect of pH on the adsorption of phosphate onto biochar derived from anaerobically digested sugar beet tailings and concluded that the optimum pH for phosphate removal by the biochar should be around 5.2, where phosphate exists in the form $H_2PO_4^-$.

Sorption kinetics studies have shown that fly ash and furnace slag with a very small particle diameter (about 0.03 mm in average) need only 3 to 5 h to reach equilibrium (Agyei *et al.*, 2000). A study of the P removal efficiency of apatite-containing materials and graymont limestone with larger particle diameter (2.5-10 mm) however, showed a two to threefold increase in P sorption from 24 to 96 hours (Bellier *et al.*, 2006). Studies on time for maximum adsorption onto biochar derived from anaerobically digested sugar beet tailings reached equilibrium after 24 hours. A related research conducted by Zhang *et al.* (2013) using cotton wood biochar indicated that the adsorption of phosphate showed rapid kinetics and reached equilibrium within 1 hour. This means that different biochar types may have different properties and therefore have different adsorptive characteristics.

Rice straw and husk, sawdust and cocoa pod abound in Ghana. These materials can easily be charred anaerobically into biochar to be used to remove nutrients such as phosphate. The P ladened biochar could then be used to enrich the P deficient soils of Ghana. To be able to achieve this, it is imperative to address some key research questions in relation to the phosphate adsorptive characteristics of the biochar prepared from rice straw, rice husk cocoa pod and saw dust:

i. What is the adsorption maximum for each of the biochar types to be prepared from the four different feedstock?
ii. What is the shaking time that will give maximum adsorption for each of the biochar types?

iii. What is the optimum pH for maximum adsorption?

iv. What is the mechanism of adsorption of P on each biochar type?

1.2 Justification

Converting rice straw, rice husk, sawdust and cocoa pod, which abound in Ghana as waste into biochar will enhance the materials' usefulness as tools for improving soil productivity especially in tropical soils. Furthermore, understanding the adsorptive characteristics of phosphate on these four biochar types is necessary if low cost appropriate technologies are to be developed for phosphate removal from industrial, municipal and domestic effluents using biochar from sawdust, rice husk and straw and cocoa pod.

1.3 Hypothesis

H_o: Biochar prepared from sawdust, rice husk and straw and cocoa pod will not have different sorption affinity for phosphate.

H_A: Biochar prepared from sawdust, rice husk and straw and cocoa pod will have different sorption affinity for phosphate.

1.4 Objectives

The objectives of the study were to:

i. determine the shaking time that will give the maximum adsorption of phosphorus.

ii. determine the optimum pH for maximum adsorption of phosphorus on biochar types to be prepared from sawdust, rice husk and straw and cocoa pod

iii. determine which of the four biochar types is best suited for adsorption of phosphorus

iv. elucidate the adsorption mechanism of phosphorus on the four biochar types.

CHAPTER TWO

LITERATURE REWIEW

2.1 Definition and Scope of Sorption

Persistence of nutrients such as phosphate, nitrate and organic pollutants in topsoil and aquatic systems and the evaluation of the degree of contamination are problems of particular environmental concern (Delle, 2001). Knowledge of the sorption characteristics of the pollutants and adsorbents is necessary to investigate these pollutants (Delle, 2001).

Sorption refers to any removal of a compound from solution to a solid phase (Sposito, 2008). The inverse process which involves the release of ions or molecules from solid phase into solution is defined as desorption (Thompson and Goyne, 2012). These definitions are universally applicable and useful when one has no knowledge of the actual sorption mechanism. Depending on the sorption mechanism, the process can be categorised into adsorption, absorption and precipitation. Adsorption is the accumulation of chemicals at the solid-liquid interface whereas absorption involves the accumulation of molecules within existing solid and the incorporation of substances within an expanding three-dimensional solid is precipitation (Thompson and Goyne, 2012; Delle, 2001).

Terms frequently used when discussing sorption processes are ‘sorptive’, ‘sorbate’, and ‘sorbent’. The adsorbing/absorbing solid phase is called the sorbent whiles the solute in the liquid phase that could be potentially sorbed is known as sorptive, and the constituents that accumulate on or within a solid are termed sorbate (Thompson and Goyne, 2012; Delle, 2001).

Sorptive is categorised into anionic, cationic and zero charged depending on the charge. Anionic sorptives are negatively charged because they have more electrons than protons. Common

examples are PO_4^{3-}, and NO^{3-}. Cationic sorptives are positively charged because they have fewer electrons than protons such as the divalent cations Ca^{2+}, Zn^{2+} and Pb^{2+}. Zero charged/uncharged organic sorptives exhibit a range of polarities (non-polar to polar) based on the distribution of electrons across the molecule (Thompson and Goyne, 2012). Liu *et al.* (1998), pointed out that metal-oxides are variably charged and their surfaces can become hydroxylated when exposed to water and assume anionic, neutral, or cationic forms based on the degree of protonation as shown below

$$\equiv M\text{-}O^- \Leftrightarrow \equiv MOH \Leftrightarrow \equiv MOH_2^+ \qquad \textbf{(Eqn 2.1)}$$

Where = M represents a metal bound at the edge of a crystal structure, which varies as a function of solution pH. Variably charged minerals adopt a net positive surface charge at low pH and a net negative surface charge at high pH (Qafoku *et al.*, 2004; Thompson and Goyne, 2012). Variations in the abundance, surface area and chemical composition of sorbents significantly influence the sorption characteristics.

2.2 Adsorption

Adsorption is a mass transfer process that involves the accumulation of substances at the interface of two phases, such as, liquid-liquid, gas-liquid, gas-solid, or liquid- solid interface (Grassi *et al.*, 2012). The substance being adsorbed is the adsorbate and the adsorbing material is termed the adsorbent. Properties of adsorbates and adsorbents are quite specific and depend upon their constituents. The constituents of adsorbents are mainly responsible for the removal of any particular pollutants (Khattri and Singh, 2009). If the interaction between the solid surface and the adsorbed molecules has a physical nature, the process is called physi-sorption. In this case, the attraction interactions are van der Waals forces and as they are weak, the process results are reversible (Grassi *et al.*, 2012). On the other hand, if the attraction forces between adsorbed

molecules and the solid surface are due to chemical bonding, the adsorption process is called chemisorption. Contrary to physi-sorption, chemisorption occurs only as a monolayer and substances chemisorbed on solid surface are hardly removed because of stronger forces of adsorption. Under favourable conditions, both processes can occur simultaneously or alternatively (Grassi *et al.*, 2012).

2.2.1 Factors affecting adsorption

The sorption of phosphate, nitrate and other organic substances on a natural solid is a very complicated process, which involves many sorbent properties, besides the physico-chemical properties of the chemical itself (Delle, 2001). Processes of adsorption are affected by factors such as surface area, nature and initial concentration of adsorbate, solution pH, temperature, interfering substances, and nature and quantity of adsorbent.

2.2.1.1 Effect of surface area

Adsorption is a surface phenomenon and the extent of adsorption is proportional to the specific surface area of the adsorbent. Surface area is defined as that portion of the total surface area that is available for adsorption (Naeem *et al.*, 2007; Grassi *et al.*, 2012). According to Grassi *et al.* (2012) the more finely divided and more porous the adsorbent is, the greater the amount of adsorption accomplished per unit weight of the solid adsorbent. The component of the adsorbent that contributes most to surface area is the pores of molecular dimensions. The maximum amount of adsorption is proportional to the surface area within pores that are accessible to the adsorbate (Delle, 2001). Surface areas range from a few hundred to more than 1500 m^2/g, but not all of these are accessible to the aqueous adsorbate. A relatively large volume of micropores generally corresponds to a large surface area and a large adsorption capacity for small molecules, whereas a

large volume of mesopores (diameter between 2 and 50 nm) and macropores (diameter > 50 nm) are usually directly correlated to capacity for large molecules (Delle, 2001).

2.2.1.2 Effect of concentration and dose of adsorbate

Adsorption process can be affected by the concentration of organic and inorganic compounds. Anbia and Hariri (2010) pointed out that the initial concentration provides an important driving force to overcome all mass transfer resistance of the adsorbate between the aqueous and solid phases. Concentration determines the capacity factor of the adsorption (Rumhayati *et al.*, 2012). According to Rumhayati *et al.* (2012), phosphate adsorption on acrylamide-ferrihydrite gel is higher at relatively low concentration because at higher concentrations there is interaction amongst the ions thereby decreasing affinity of the ions to be sorbed.

Quantity of adsorbent also plays a significant role in the adsorption process because this determines the capacity of the adsorbent for a given initial ion concentration (Mostafapour *et al.*, 2013). There is increase in removal efficiency at initial stage because of the greater availability of the exchangeable sites or surface area at the higher concentrations of the adsorbent (Pandey *et al.*, 2009; Kaczala *et al.*, 2009). Increase in the efficiency of removal may be attributed to the fact that with an increase in the adsorbent dose, more adsorbent surface or more adsorption spots are available for the solute to be adsorbed (Li *et al.*, 2012; Mostafapour *et al.*, 2013). The rate of adsorption depends upon the uncovered surface available for adsorption. Initially, the whole surface is uncovered and therefore the rate of adsorption increases whereas as the covered surface increases, the rate of adsorption is decreased. Ultimately, a stage is reached when there is no more adsorption with any further addition of adsorbent, and at that time, the adsorption process is said to be at equilibrium (Mostafapour *et al.*, 2013).

2.2.1.3 Effect of pH

The pH of solutions affects the extent of adsorption because the distribution of surface charge of the adsorbent can change thus varying the extent of adsorption according to the adsorbate functional groups (Gao and Pedersen, 2005; Putra *et al.*, 2009; Grassi *et al.*, 2012). According to Yao *et al.* (2011), adsorption of phosphate onto digested sugar beet tailings biochar depends on initial solution pH with maximum pH occurring at pH 4. Increasing solution pH higher than the optimum value may trigger polynuclear interactions that may consume more adsorption sites (Yao *et al.*, 2011). They added that the optimum pH for phosphate removal by colloidal and nano-sized MgO on biochar surface should be around 5.2, where phosphate exists in the form $H_2PO_4^-$.

2.2.1.4 Effect of time

Contact time is one of the most important parameters for maximum adsorption. Adsorption on an adsorbent from the aqueous phase involves three steps: (i) the transport of the adsorbate from the bulk phase to the exterior surface of the adsorbent (film diffusion), (ii) the transport into the adsorbent by pore diffusion and/or surface diffusion (intra-particular diffusion) and (iii) the adsorption on the surface of the adsorbent. The slowest of these steps determines the overall rate of the adsorption process (Kolodynska *et al.*, 2012). The adsorption capacity and removal efficiency significantly increase during the initial adsorption stage and then continue to increase at a relatively slow speed with contact time until a state of equilibrium is released (Mostafapour *et al.*, 2013).

Phosphorus sorption processes are complicated and usually consist of fast sorption reactions followed by slow processes (McGechan and Lewis, 2002; Cucarella and Renman, 2009). Equilibrium may be established after minutes, hours, days, or even months depending on the type of material used, the material-to-solution ratio, initial P concentration, agitation, and temperature

(Cucarella and Renman, 2009). The time needed to reach equilibrium depends strongly on the particle size of the material. Sorption kinetics studies have shown that fly ash and furnace slag with a very small particle diameter (about 0.03 mm in average) need only 3 to 5 hours to reach equilibrium (Agyei *et al.*, 2002). On the other hand, a study of the P removal efficiency of apatite-containing materials and graymont limestone with larger particle diameter (2.5-10 mm) showed a two- to threefold increase in P sorption from 24 to 96 hours (Bellier *et al.*, 2006).

According to Cucarella and Renman (2009), the higher the porosity of a material, the higher the specific surface area and sorption capacity, but at the same time, the longer the contact time needed to reach equilibrium due to slow P movement processes such as intraparticle diffusion. A study by Zhang *et al.* (2013) revealed that the adsorption of phosphate on cotton wood biochar showed rapid kinetics and reached equilibrium within 1 hour, which is faster than that of other types of biochars that reached equilibrium after 24 hours. (Das *et al.*, 2006; Yao *et al.*, 2011).

Adsorbate is adsorbed easily on the surface (macropores) of the adsorbent, and therefore rapid adsorption occurs on the macropores surface. In contrast, in the interior (micropores) of the adsorbent, the adsorbate would be adsorbed by a pore and/or surface diffusion mechanism, resulting in a slower adsorption. After maximum adsorption, a further increase in contact time has insignificant effect on the amount of adsorption. Generally, the removal rate of sorbate is rapid initially, but it gradually decreases with time until it reaches equilibrium (Cengiz and Cavas, 2008; Gulnaz *et al.*, 2011; Mostafapour *et al.*, 2013).

2.3 Forces of adsorption

Forces responsible for adsorption reactions include physical forces, chemical forces, hydrogen bonding, electrostatic attraction, coordination reaction and ligand exchange. It is believed that hydrogen bonding can qualify either as a chemical or physical process. On the other hand,

protonation, electrostatic attraction, ion exchange and coordination can be considered as chemical adsorption process. Weber *et al.* (1991) summarized the possible interactions between solute and sorbent into three categories of sorption: physical, chemical, and electrostatic.

2.3.1 Physical adsorption

Physical sorption processes involve interactions between dipole (permanent or induced) moments of sorbate and sorbent molecules. The most important force in the physical adsorption process is the Van der Waals force. Van der Waals forces become essential at close distances between interacting molecules and decrease rapidly with distance. Their effect is greatest when ions are in close contact. The less intimate the contact between the solute and the adsorbent surface, the smaller the rate of adsorption (Webb, 2003). This implies that small and spherically shaped ions will be in close contact with the surface than larger ions. Adsorption of organic anions or basic organic compounds by Van der Waals forces occur when the surface acidity of the adsorbent is more than two pH units lower than the dissociating constant of the adsorbent (Webb, 2003). Physical adsorption is accompanied by a decrease in free energy and entropy of the adsorption system and, thereby making the process exothermic (Grassi *et al.*, 2012).

2.3.2 Chemical adsorption

Chemical interactions occur through protonation. Protonation occurs at the colloidal surface in the hydration shells of cations and in the solution phase. Chemical adsorption is a significant force in the adsorption of anions and organic compounds basic in nature because of the development of positive charge. For example, ammonia (NH_3) ions are chemisorbed by clays in the form of NH_4^+, which is the pronated form of NH_3. Studies have shown that protonation of organic compounds in the interface is affected by the exchangeable cation, basicity of the adsorbate, water content of the adsorbing medium and surface acidity. However, the surface acidity is the most important factor

in providing protons necessary for protonation of anions and basic organic compounds (Moreno-Castilla, 2004; Webb, 2003).

2.3.2.1 Hydrogen bonding

Hydrogen bonding is an adsorption process where a hydrogen atom acts as the connecting linkage and is related to protonation. However, protonation involves a full charge transfer from an electron donor (base) to the electron acceptor (acid), whereas hydrogen bonding is a partial transfer (Moreno-Castilla, 2004). Organic compounds containing functional groups such as N-H, OH, COOH groups are adsorbed by formation of hydrogen bonds between the functional groups and oxygen.

2.3.2.2 Electrostatic bonding

Electrostatic bonding is made possible because of the electrical charge on the colloidal surface. Two negatively charged ions in contact would be expected to repel as in the case of organic compounds and clay, however, protonation of the organic substance may convert them into positively charged ions. Protonation in this case is possible by hydronium ions on the exchange site. When an adsorbed organic ligand exchanges for an inorganic cation, it is known as ligand exchange (Kah, 2007; Tan, 2011).

2.3.2.3 Coordination reaction

It is adsorption through coordinate covalent bonding when a ligand donates an electron pair to a metal ion. The resulting compounds are called coordination compound or organo-metal complex. Coordination compounds are substances containing a central atom usually metal surrounded by a cluster of organic ligands (Tan, 2011).

2.4 Sorption Isotherms

Sorption isotherms describe how an adsorbate interacts with an adsorbent. The isotherm provides a relationship between the concentration of a substance in solution and the amount adsorbed on the solid phase when both phases are in equilibrium. In a solid-liquid system, adsorption results in the removal of solutes from solution and their accumulation at solid surface (Stumm and Morgan, 1996). The solute remaining in the solution reaches a dynamic equilibrium with the adsorbed on the solid phase.

2.4.1 Quantity adsorbed (qt)

The amount of adsorbate that can be taken up by an adsorbent as a function of both temperature and concentration of adsorbate, and the process, at constant temperature, can be described by an adsorption isotherm according to the general equation (Grassi *et al.*, 2012).

$$\boldsymbol{qt = \frac{(C_o - C_t)V}{m}} \qquad (\boldsymbol{Eqn.2.2})$$

Where qt (mg/kg) is the amount of adsorbate per unit mass of adsorbent at time t, C0 is the initial concentration of adsorbate at time t and Ct (mg/L) is the equilibrium concentration of adsorbate, V is the volume of the solution (L), and m is the mass of adsorbent (g).

The equilibrium adsorption data is analyzed by several statistical models chief of which are mostly the Langmuir (1918) and Freundlich (1926) isotherm models.

2.4.2 Langmuir isotherm

The Langmuir isotherm model is valid for monolayer adsorption onto surface containing a finite number of identical sorption sites. Sorption isotherms fitted to a Langmuir model, assumes that the sorbent surface has a finite number of sorption sites and the sorptive energy is the same in all the sites (i.e. all sites are identical). Furthermore, each sorptive site is occupied only by a single

molecule and there are no interactions between the sorbed molecules (Mesa and Kurt, 2011). The Langmuir model is presented by the equation 2.3:

$$\frac{\mathbf{qe}}{\mathbf{qm}} = \frac{\mathbf{bCe}}{(\mathbf{1} + \mathbf{bCe})} \qquad (\mathbf{Eqn.2.3})$$

Where qe (mg/kg) is the amount of adsorbate per unit mass of adsorbent at equilibrium, Ce is the liquid-phase concentration of the adsorbate at equilibrium (mg/L), qm is the maximum adsorption capacity (mg/kg) and b is the Langmuir constant related to the energy of adsorption (L/mg).

A plot of Ce/qe against Ce is used to determine the sorption maximum and the energy of adsorption.

The b parameter is directly related to surface energy, thus increasing surface energy increases the probability of adsorption at a given pressure. It is inversely related to temperature, which, when increased, increases molecular energy and decreases the probability of adsorption at a given pressure (Webb, 2003).

2.4.3 Freundlich isotherm

Freundlich isotherm is used to describe the adsorption characteristics for heterogeneous surface (Cooney, 1999; Dada *et al.*, 2012). The Freundlich model is described by the equation below:

$$\mathbf{Qe} = \mathbf{K_F Ce}^{1/\mathbf{n}} \qquad (\mathbf{Eqn.2.4})$$

Where K_f = Freundlich isotherm constant (mg/g), n = adsorption intensity, Ce = the equilibrium concentration of adsorbate (mg/L), Qe = the amount adsorbed per gram of the adsorbent at equilibrium (mg/g).

$$\boldsymbol{log\ Qe = logK_F + {}^{1}/_{n}\, logCe} \qquad (\boldsymbol{Eqn.2.5})$$

$\log K_F$ is the intercept and 1/nlogCe is the slope.

The constant Kf is an approximate indicator of adsorption capacity, whereas 1/n is a function of the strength of adsorption in the adsorption process (Voudrias, 2002; Dada, 2012). If n = 1 then the partition between the two phases are independent of the concentration (Dada *et al.*, 2012). If value of 1/n is below one it indicates a normal adsorption. On the other hand, 1/n being above one indicates cooperative adsorption (Mohan and Karthikeyan, 1997). According to Dada *et al.* (2012), as the temperature increases, the constants k and n change to reflect the empirical observation that the quantity adsorbed rises more slowly and higher pressures are required to saturate the surface. The model that has a higher coefficient of determination (R^2) value is used to describe the adsorption.

2.4.4 Dual–mode model (DMM) (Langmuir-Freundlich)

Sorption isotherms can also be described by the Dual–mode model (DMM). The DMM is a Langmuir-Freundlich model which includes solid-phase dissolution (partitioning) and is described by a linear term and a hole-filling component characterized by a Langmuir term. The DMM is given by:

$$qe = K_D Ce + \frac{Q_{max} LCe}{KLD + Ce} \qquad (Eqn.2.6)$$

Where qe (mg/kg) is the amount of adsorbate per unit mass of adsorbent at equilibrium, Ce is the liquid-phase concentration of the adsorbate at equilibrium (mg/L), Kd is the dissolution domain partition coefficient, and Q_{max}L and KLD are the capacity and affinity coefficient, respectively, of the hole-filling domain (Huang *et al.*, 2003; Lou *et al.*, 2011).

Zeng *et al.* (2013), showed that the isotherm for phosphate sorption fits the Langmuir model much better, with correlation coefficients ranging from 0.947 to 0.964. This result differs from previous

reports showing that phosphate sorption on biochar materials fits the Freundlich isotherm better than the Langmuir model with phosphate precipitation being the mechanism of adsorption (Yao *et al.*, 2011).

2.5 Application of adsorption in environmental management.

Adsorption plays an important role in environmental management. The concern of eutrophication and need for alternative cheaper source of plant nutrients has driven local state, federal agencies, municipalities, and private industry to invest in research concerning nutrient recovery (Streubel, 2011). Different forms of technologies and methods have been used for phosphorus recovery. Some of these technologies include precipitation with metals and biological methods involving the use of microorganisms.

Metal ions have been used in different environments depending on the pH to precipitate P (Streubel, 2011). For example, aluminum is very effective in precipitating P at pH of 3.6, whereas calcite is used in high pH systems (pH 9.0) (de–Bashan and Bashan, 2004). Iron, aluminium, magnesium, calcite and products from other industrial wastes such as a slag, or oxides from steel production have been added to wastewater or sludge phosphorus form complexes with these metals forming aggregates which precipitate allowing the resulting solid to be collected (Banu *et al.*, 2008; Streubel, 2011). The precipitate obtained is, however, not useful for farming purposes because of high metal toxicity (Delhaize and Ryan, 1995).

The growing concerns to get cheaper sources of phosphorus, which are the primary drivers of good plant nutrition, continue to trigger a lot of research into nutrient recovery. As a result, scientists developed the use of activated carbon (AC) from various sources for P removal. According to Bhargava and Sheldarkar (1993), activated carbon from Tamarind (*Tamarindus indica*) nutshell was found to successfully remove 95% of the P from a standard solution through adsorption. Other

materials such as powdered activated carbon from hardwood were used to remove P from industrial wastewater effluent (Meidl, 1997).

Intensive research has shown that the adsorption of phosphate ions depends upon the concentration and accessibility of cations found in the ash. Immense studies were directed toward the effects of metal ion concentrations in fly ash as it exhibited a massive potential to remove phosphate compounds from wastewater (Lu *et al.*, 2009; Agyei *et al.*, 2002; Oguz, 2005; Zhang, 2007; Streubel, 2011). However, the expense of the activation of charcoal has prevented the use of activated charcoal in environmental management programs.

Biochar is another porous black material obtained from pyrolysis of organic materials currently receiving a lot of attention for its adsorptive capacities and ability to adsorb phosphate and nitrate (Steubel, 2011). As the focus of nutrient removal technology turns towards recycling, the ability of the resulting co-products to be used as a fertilizer supplement will be a driving force (de–Bashan and Bashan, 2004; Streubel, 2011).

2.6. Biochar

2.6.1 History and origin

Biochar is a carbon (C) rich product derived from the pyrolysis of organic material at relatively low temperatures (<700 °C) (Lehmann and Joseph, 2009). Use of biochar as a soil amendment has been around since the early 1800s (Lehmann *et al.*, 2006; Lehmann and Joseph, 2009). The interest in biochar as a soil amendment was prodded by studies of Amazonian soils (Terra Preta) where the presence of charcoal was associated with significant improvements in soil quality such as soil organic matter, nutrient concentrations and increases in crop yields (Glaser *et al.*, 2002). Application of chars and ash derived from cooking fires, plus other debris that included bones and manure to soil could be traced to the early residents (450 Before Common Era to 650 Common

Era) of the Amazon River Basin (Sombroek, 1966). Observed improvements in chemical and physical properties of these soils have persisted for hundreds to thousands of years (Lehmann, 2007). This has contributed to the current global high interest in biochar.

Biochar is produced through a thermochemical process under low oxygen conditions known as pyrolysis (Duku *et al.*, 2011). Various types of biomass ranging from agricultural crop residues, forestry residues, wood waste, organic portion of municipal solid waste (MSW) and animal manures have been proposed as feedstock for biochar production (Duku *et al.*, 2011). Suitability of each type of biomass as feedstock is dependent on the nature, chemical composition, environmental, economic, and logistical factors (Verheijen, 2010; Duku *et al.*, 2011). The feedstock type and pyrolysis conditions are the main factors controlling the physical and chemical properties. Biochar is highly recalcitrant in soils, with reported residence times for wood biochar being in the range of hundreds to thousands of years, i.e. approximately 10-1000 times longer than residence times of most soil organic matter (SOM) (Verheijen, 2010).

2.6.2 Pyrolysis

Pyrolysis comes from the Greek word 'pyro' meaning fire and "lysis" meaning decomposition or breaking down into constituent parts (Verheijen *et al.*, 2010). Pyrolysis is defined as the chemical decomposition of an organic substance by heating in the absence of oxygen (Duku *et al.*, 2011; Verheijen *et al.*, 2010). Pyrolysis is the first step in combustion and gasification. Gasification involves the burning of biomass at temperatures above 800 ^{o}C in the presence of oxygen yielding syngas for energy production and a little biochar (Streubel, 2011). The process of pyrolysis breaks down the polymeric building blocks of the biomass consisting mainly of cellulose, hemicellulose and lignin through processes such as cross-linking, depolymerisation and fragmentation at various temperatures (Duku *et al.*, 2011). Biomass pyrolysis transforms the organic materials into three

different products primarily: gas often referred to as non-condensable volatiles, liquid (bio- oil) often classified as condensable volatiles and solid in different proportions depending upon both the feedstock and the pyrolysis conditions used (Duku *et al.*, 2011; Verheijen *et al.*, 2010).

Feedstock type, nature, and composition particularly the lignin and ash contents, and the pyrolysis process conditions such as temperature, pressure, heating rates, particle size and heat integration determine the product yields of pyrolysis (Demirbas, 2001). In the same way, biochar quality, characteristics and composition are predominantly determined by the type, nature and origin of the feedstock, as well as the pyrolysis conditions (Verheijen *et al.*, 2010, Zhang *et al.*, 2008). Evaluation of biochar yield from different feedstock has shown that biomass with high lignin content has high biochar yields because of the stability of lignin to thermal degradation (Demirbas, 2004). Biochar from crop residues such as maize, rice straw, rye and manures are generally finer and less robust with low mechanical strength and hence low biochar yield (Duku *et al.*, 2011).

Pyrolysis can be classified as slow, intermediate and fast depending upon the pyrolysis condition and processes (Brown, 2009; Sohi *et al.*, 2009; Duku *et al.*, 2011). According to Duku *et al.* (2011), the energy required to drive the pyrolysis process can be supplied directly through the heat of reaction, or by flue gases from combustion of by-products and/or feedstock, and indirectly by flue gases through the reactor wall, or by heat carrier other than flue gases such as sand, metal spheres, etc. Among the pyrolysis processes, slow pyrolysis and intermediate pyrolysis give higher biochar yields, while fast pyrolysis gives higher liquid yields. (Duku, 2011). Factors which enhance high biochar yields are the high lignin, ash and nitrogen contents in the biomass, low pyrolysis temperature (<400 °C), high process pressure, long vapour residence time, extended vapour/solid contact, low heating rate, large biomass particle size, and optimised heat integration (Brownsort, 2009; Demirbas, 2004; Duku, 2011).

Investigations carried out so far on biochar production has revealed that chars made from herbaceous feedstock such as rice straw, husk, switch grass, peanut hulls, etc. have lower carbon contents, higher nitrogen contents, and higher pH than chars made from woody feedstock (Novak *et al.*, 2009; Granatstein *et al.*, 2009; Streubel, 2011). Feedstock and pyrolysis temperature determines the pH and is attributed to the chemical cracking of hemicellulose and cellulose during pyrolysis. At pyrolysis temperature between 300 to 600 ^{o}C, organic acids and phenolic substances are created and alkali salts are formed that raise the pH of the biochar (Streubel, 2011; Shinogi and Kanri, 2003). The higher pH of herbaceous biochar give them a greater liming impact per tonne of biochar added to soil, increasing soil pH 0.5 - 1.0 pH units depending on soil type. High pH of biochar is also related to the concentration of Ca and Mg as higher Ca concentrations can serve as buffers (Chan *et al.*, 2009; Gaskin *et al.*, 2008).

2.7 Physical and chemical characterisation of Biochar

Biochar composition is highly heterogeneous, containing both stable and labile components (Sohi *et al.*, 2009; Verheijen, 2010). The primary factor controlling the chemical and physical properties of biochar is the feedstock. For agricultural related use of biochar, seven properties have been identified to determine the quality of biochar. These properties include pH, volatile compound content, and ash content, water holding capacity, bulk density, pore volume, and specific surface area (Sohi *et al.*, 2009; Amonette and Joseph; 2009; Krull *et al.*, 2009). The elemental composition of biochar is greatly affected by the processing temperature and pyrolysis residence time. According to Kuwagaki and Tamura (1990), increase in pyrolysis temperature is associated with a corresponding increase in pH of biochar. In the same way, surface area of biochar is also greatly controlled by temperature. For example, bagasse carbonization at different temperatures produced

biochar with different specific surface area. The specific surface area at 600 °C was 270 m^2/g but jumped to 322 m^2/g at 700 °C (Ueno *et al.,* 2007).

Temperature effect has led to suggestions that biochar created at low temperature may be suitable for controlling the release of fertilizer nutrients whilst high temperature biochar would be more suitable for use as activated carbon. However, the hydrophobic nature of the surface of low temperature biochar may limit their capacity to store water in soil (Ogawa *et al.,* 2006; Day *et al.,* 2005; Sohi *et al.,* 2009). The porous structure of biochar is positively correlated to its soil water holding and adsorption capacity (Day *et al.,* 2005; Ogawa *et al.,* 2006; Sohi *et al.,* 2009). Studies have shown that carbon content in biochar range between 172 to 905 gkg^{-1} (Verheijen, 2010; Chan and Xu, 2009). The C: N (carbon to nitrogen) ratio in biochar has been found to vary widely between 7 and 500 with implications for nutrient retention in soils. The C: N ratio has been commonly used as an indicator of the capacity of organic substrates to release inorganic N when incorporated into soils (Chan and Xu, 2009).

Elemental analyses of biochar had shown that mineral content of the feedstock remains in the resulting biochar, where it is concentrated due to the loss of C, H and O during pyrolysis (Amonette and Joseph, 2009). Biochar derived from herbaceous biomass and manures have N, P, K and S contents greater than that produced from woody feedstock. Total N in biochar has also been shown to vary between 1.8 and 56.4 gkg^{-1}, depending on the feedstock (Chan and Xu, 2009; Verheijen, 2010). According to Streubel (2011), most of the N and S are lost during pyrolysis as temperatures increase from 350 to 600 °C. Shinogi and Kanri (2003), estimated that about 60 to 80% of N was lost during pyrolysis of sugar cane bagasse, rice (*Oryza sativa*) husks, sewage sludge, and cattle manure. This is because as pyrolysis temperatures increases, the N forms pyridine-like complexes that reduce its availability (Bagreev *et al.,* 2001). Decrease in N concentration can be attributed to

volatilization during heating and that some of the N–containing structures in the biochar (e.g., amino acids, amines, amino sugars) are condensed into recalcitrant forms and therefore may be unavailable for plant use (Cao and Harris, 2010).

The complex and heterogeneous chemical composition of biochar is extended to its surface chemistry, which in turn explains the way biochar interacts with a wide range of organic and inorganic compounds in the environment (Verheijen *et al.*, 2010). During pyrolysis, there is breaking and rearrangement of the chemical bonds in the biomass resulting in the formation of numerous functional groups (e.g. hydroxyl –OH, amino–NH_2, ketone –RC(=O)R, ester – (C=O) – OR, nitro –NO_2, aldehyde –(C=O)H, carboxyl –(C=OOH). They occur predominantly on the outer surface of the grapheme sheets and surfaces of pores (Verheijen *et al.*, 2010). Some of these groups act as electron donors, while others as electron acceptors. These properties have been utilized for use in recovery of nutrients and metals from aqueous solutions, wastewater, etc. (Amonette and Joseph, 2009). Transmission Electron Microscopy showed that prepared biochar surface is unshaped, coarse, and irregular (10–30 µm length). Energy Dispersive X–ray (EDX) showed that the surface composition of biochar contain a great deal of carbon. Fourier Transform Infrared spectroscopy (FTIR) studies have indicated the presence of organic functional groups on the surface of biochar (Zeng *et al.*, 2013).

The FTIR spectral analysis by Han *et al.* (2013), revealed the principal surface functionalities of rice straw biochar to be at five bands at wave lengths 3374, 1587, 1378, 1090, and 791 cm^{-1} attributed to hydroxyl (–OH) stretching, CO-C stretching of secondary hydroxyl, aliphatic CH3 deformation, and aromatic C=C ring and COO- group stretching, respectively. The 1378 cm^{-1}, band has been attributed to aliphatic CH_3 deformation (Harvey *et al.*, 2011; Han *et al.*, 2013) or O–H/C–H bending of hydroxyl, acid, phenol and methyl (Fu *et al.*, 2009).

2.8. Functions of biochar

Carbon sequestration is the primary driver for considering the application of biochar to the soil. Decomposition of organic matter contributes to the release of CO_2 into the atmosphere, which implies that turning biologically derived organic matter into a highly stabilised form through pyrolysis can decrease CO_2 emission from soil as the rate of decomposition is lowered (Sohi *et al.,* 2009). It has been reported that currently biomass burning accounts for 10% of global CH4 emissions and 1% of N_2O although charcoal production is part of these emissions and therefore a shift to pyrolysis-based systems would decrease, if not eliminate, them. This means that biochar offers a huge potential for climate change mitigation (Crutzen and Andreae, 1990; Sohi *et al.,* 2009; Woolf, 2008).

Addition of biochar to soil dramatically darkens the colour of soil, especially in soils that are low in organic matter (Sohi *et al.,* 2009). The dark nature of these soils increases absorption of solar energy depending on the water content and plant cover and with a concomitant increase in soil temperatures. This will affect rate processes, enhancing the cycling of nutrients and potentially extending the growing season in seasonal climates (Krull *et al.,* 2004; Sohi *et al.,* 2009). Although, the purpose of biochar application might not simply be to attain a greater yield, Sohi *et al.* (2009), conceptualize three main mechanisms to explain how biochar might benefit crop production:

i. Direct modification of soil chemistry through its intrinsic elemental and compositional make up,
ii. Providing chemically active surfaces that modify the dynamics of soil nutrients and
iii. Modification of physical character of the soil in a way that benefits root growth and/or nutrient and water retention and acquisition.

Evidence from previous works on rates of biochar application suggests that at least for some crop and soil combinations, moderate additions of biochar are usually beneficial and in very few cases negative. It is also evident that higher biochar application rates seemed to inhibit plant growth (Ogawa *et al.*, 2006; Sohi *et al.*, 2009). However, combination of higher biochar application rates alongside NPK fertilizer increased crop yield on tropical Amazonian soils (Steiner *et al.*, 2007) and semi-arid soils in Australia (Ogawa *et al.*, 2006; Sohi *et al.*, 2009).

Beneficial characteristics of biochar as a soil amendment include high cation exchange capacity (CEC; 40 to 80 cmol/kg, high surface area (51 to 900 m^2/g), increased soil pH and water holding capacity. The material has high affinity for micro- and macro- plant nutrients (Lehmann, 2007; Gaunt and Lehmann, 2008; Lehmann and Joseph, 2009; Streubel, 2011).

Research has also shown that in many tropical and subtropical soils, addition of biochar increases exchangeable bases, CEC, and nutrient availability, decreases soil density and improves water-holding capacity (Liang *et al.*, 2006). The incorporation of biochar into soil can alter soil physical properties such as texture, structure, pore size distribution and density with implications for soil aeration, water holding capacity, plant growth and soil workability (Downie *et al.*, 2009; Verheijen, 2010; Sohi *et al.*, 2009).

2.9. Factors affecting adsorption on biochar

The behaviour of biochar following its application to the soil has prompted a lot of research on its sorption abilities. Pyrolysis temperature and feed stock are the main factors governing the properties of biochar and consequently their adsorptive characteristics (Tang *et al.*, 2013; Sohi *et al.*, 2009; Duku *et al.*, 2011). The increase of pyrolysis temperature will lead to the increase of surface area of biochar, which facilitates higher sorption of chemicals such as pesticides and other organics (Zeng *et al.*, 2013). Increase in pyrolysis temperature may improve the sorption ability of

biochar for nitrate and phosphate (Yao, *et al.*, 2012). For example, biochar made from wheat residue at 500-700 °C was well carbonized and its surface area was relatively high (>300 m^2/g), whereas chars formed at 300-400 °C were partially carbonized and had a lower surface area (<200 m^2/g). The former therefore exhibited high sorption capability for organic compounds (Chun *et al.*, 2004).

Biochars derived from various materials show different properties such as functional groups, porosity, cation exchange capacity, etc., which may have adverse effect on their adsorptive properties (Tang *et al.*, 2013; Kolodynska *et al.*, 2012; Yao *et al.*, 2011). Zeng *et al.* (2013), conducted a research on the sorption of phosphate from aqueous solution by biochars derived from *Salix rosthornii Seemen, Thalia dealbata, Vetiveria zizanioides,* and *Phragmites sp*., and under different temperatures (500, 600, and 700 °C). They found out that the cation exchange capacity and specific surface area of biochar varied with both plant species and pyrolysis temperature. The magnesium (Mg) content of biochar derived from *T. dealbata* was higher than that of the other plant biochars and had the highest sorption capacity for phosphate. They concluded that Mg was more responsible for P sorption than surface area.

Abundance of organic functional groups on the surface of biochar means that phosphate could also be removed by biochar through interaction with the functional groups. However, a study by Yao *et al.* (2011), indicated similarity between the FTIR spectra of the original and P-loaded biochar. They concluded that there was no evidence of adsorption of phosphate onto the surface functional groups in the P-loaded biochar.

Research has shown that addition of appropriate metal ions to the structure of the biochar should aid in creating additional basic sites on the char surface which will become positively charged in solution and attract anions to the surface (Streubel, 2011; Yao *et al.*, 2013; Yao *et al.*, 2012).

Though most of the engineered carbons, including biochar, have been reported to have limited ability to adsorb phosphate or other anionic nutrients such as nitrate (Strahm and Harrison, 2006; Yao *et al.*, 2012; Yao *et al.*, 2013). As a result, a number of techniques have been developed to modify the surface of engineered carbons to improve their affinity for negatively charged ions (Chen *et al.*, 2007; Yao *et al.*, 2013).

Recent studies suggested that biochar based composites with colloidal or nanosized MgO particles impregnated within carbon matrix have strong affinity for aqueous phosphate under various conditions (Yao *et al.*, 2011; Zhang *et al.*, 2013). According to Yao *et al.* (2013), the maximum sorption capacity of this new type of engineered biochar to phosphate can reach more than 100 mg/g, which is greater than that of any other carbon-based sorbents reported in the literature (all lower than 20 mg/g). For instance, activated carbon is the most popular engineered carbon used in separation processes; however, its reported sorption capacity to P is still lower than 15.1 mg/g even after surface modification with iron or other metal elements (Bhargava and Sheldarkar, 1993; Namasivayam and Sangeetha, 2004). The high sorption ability of the improved biochar could be attributed to the large amount of colloidal or nanosized MgO particles distributed on the carbon surfaces within the pores of the biochar matrix (Yao *et al.*, 2011; Yao *et al.*, 2013).

2.10 Mechanism of phosphate adsorption onto biochar

Considerable effort has been made towards understanding the primary mechanism of phosphate adsorption onto biochar. According to Lu *et al.* (2009), majority of phosphate removal appeared to be due to precipitation reactions. However, a reasonable level of adsorption could be achieved on the ash. Sorption of phosphate from aqueous solutions is generally governed by the surface functional group, surface area of the adsorbent and metal-ion complex formation (Zeng *et al.*, 2013). Previous studies have shown that the surface of the biochar is often negatively charged,

making it repel negatively charged ions such as phosphate (Yao *et al.*, 2011a), suggesting that the sorption of phosphate via surface chemistry should be minimal (Zeng *et al.*, 2013).

Elemental analysis indicated that large amount of calcium (Ca) and magnesium (Mg) could be present on the surface of biochar. Under alkaline conditions, the presence of Ca and Mg cations favours precipitation with phosphate (Zeng *et al.*, 2013; Gerritse, 1993; Arias *et al.*, 2001). Previous studies showed no evidence of phosphate removal by Ca, suggesting that Ca is insignificant in phosphate removal (Zeng *et al.*, 2013). Similar result was obtained by Yao *et al.* (2011b), based on the X–ray diffraction (XRD) spectra of original and P-loaded biochar. They added that the precipitation of P with Ca might not be an important mechanism for phosphate removal because some Ca in biochar was present on its surface in the form of calcite, which has a low solubility, and Ca trapped inside the biochar could not be released into the solution.

Post–adsorption characterizations using SEM-EDS, XRD, and FTIR suggested that colloidal and nano-sized MgO (periclase) particles on the biochar surface were the main adsorption sites for aqueous phosphate (Yao *et al.*, 2011b). Zeng *et al.* (2013) also suggested surface precipitation by Mg is a factor controlling adsorption of phosphate on to biochar.

Studies have shown that metal oxides show strong ability to adsorb negative charged compounds, such as phosphate, nitrate and arsenate (Manning and Goldberg, 1996; Yao *et al.*, 2011) when in contact with water. The metal oxide surface becomes hydroxylated, and thus introduces either a positive or a negative surface charge, depending on the solution pH. The charge development of MgO as a factor controlling adsorption on the biochar surface can be described in a simplified manner by

$$\mathbf{SMgO - OH_2^+ \Leftrightarrow SMgO - OH \Leftrightarrow SMgO - O} \qquad \textbf{(Eqn 2.7)}$$

Where SMgO denotes the MgO surface. The point of zero charge (PZC) of MgO is very high (PZC MgO =12 (Kosmulski, 2009; Yao *et al.*, 2011b), thus its surface is expected to be positively charged in most natural aqueous conditions (Yao *et al.*, 2011). In aqueous solution, phosphate exists in three species with pKa values of 2.12 (pKa1), 7.21(pKa2), 12.67 (pKa3). When solution pH is lower than point of zero charge of MgO, the hydroxylated MgO surface can electrostatically attract negatively charged phosphate species to form mono-, bi and polynuclear complexes (Schindler and Stuwn, 1987; Shin *et al.*, 2004; Yao *et al.*, 2011a) as shown below by Yao *et al.* (2011b).

$$\mathbf{SMgO - OH_2^+ + H_2PO_4^- \Leftrightarrow SMgOH_2PO_4 + 2H_2O,} \qquad \textbf{(Eqn 2.8)}$$

mononuclear (0.12 < pH < 9.21)

$$\mathbf{2SMgO - OH_2^+ + HPO_4\text{-}2 \Leftrightarrow (SMgO)_2HPO_4 + 2H_2O,} \qquad \textbf{(Eqn 2.9)}$$

binuclear (5.21 < pH < 10.67)

$$\mathbf{3SMgO - OH_2 + PO_4^{-3} \Leftrightarrow (SMgO)_3PO_4 + 3H_2O} \qquad \textbf{(Eqn 2.10)}$$

trinuclear (10.67 < pH < 12)

The above equations are clear prove that the pH is a key factor in adsorptive process (Yao *et al.*, 2011b).

CHAPTER THREE

MATERIALS AND METHODS

3.1 Preparation of biochar Adsorbent

Cocoa pod, saw dust, rice husk and rice straw were used as feed stock for biochar preparation. The rice husk and straw raw material were obtained from the University of Ghana, Soil and Irrigation Research Centre (SIREC), Kpong, located within the lower Volta Basin of the Coastal Savannah Agro-Ecological Zone of Ghana. Sawdust raw material was obtained from Ahinsan Kumasi in the Ashanti Region of Ghana. Cocoa pod raw material was collected from CRIG, Tafo in the Eastern Region of Ghana. These feedstock materials were then transported to the Soil Research Institute, Kwadaso Kumasi for charring in a reactor.

The cocoa pods and the rice straw being larger materials were chopped into smaller pieces to increase their respective surface area and also to facilitate drying. The various raw materials were then air dried amidst regular turning on a clean platform for about three days and then oven dried at 70 ^{o}C to reduce the moisture content before charring. The reactor was warmed for about one hour for equilibration of temperature before loading the raw materials. Charring temperature was about 450 ^{o}C. Residence time for charring was 48 and 46 hours for rice husk and sawdust, respectively and 24 hours for cocoa pod and rice straw biochar. Charring temperatures above the stated duration turned the biochar into ashes.

When charring was complete, the respective biochar samples were washed with distilled water and then air dried. Each sample was then ground in a stainless steel mill and passed through a 0.5 mm sieve to obtain a less than 0.5 mm sized fraction. This particle size fraction of each biochar type

was then further dried in an oven at 70 °C. Samples were sealed for characterization and subsequent adsorption experiments.

3.2 Biochar characterization

Parameters and their respective methods of determination used to characterize the adsorbents are listed in Table 3.1 below

Table 3. 1 Properties of adsorbents and their respective methods of determination.

PROPERTY	METHOD
pH (H_2O, 1M $CaCl_2$)	Electrometric
Electrical Conductivity	Electrometric
Total elemental analysis	Wet digestion
CEC	NH_4Acetate
AEC	KCl method
Total N	Kjeldahl method
Organic carbon	Walkley and Black
Mineral	X-ray

3.2.1 pH

Ten grams each of the biochar was weighed into separate 100 mL beakers and 50 mL of de-ionised water added at a 1:5 ratio (biochar: solution). The suspension was stirred thoroughly and allowed to stand for 30 minutes to equilibrate. After calibrating a Hanna H19017 microprocessor pH meter electrode was immersed into the supernatant and the samples' pHs recorded. The same procedure was carried out using 0.01M $CaCl_2$ at a ratio of 1: 10 ratio (biochar: solution).

3.2.2 Cation exchange capacity

Ten grams of biochar samples were weighed into an extraction bottle and 100 mL of 1 M ammonium acetate solution added. The bottle with its content was shaken for 30 minutes on a mechanical shaker. The content was then filtered through a No. 42 Whatman filter paper and the sample leached four times with 25 mL of methanol to wash off excess ammonium. Thereafter, another 25 mL of 1 M acidified potassium chloride was used to leach the biochar samples four times. A 5 mL aliquot of the leachate was taken into a Markham distillation apparatus and 5 mL of 40% NaOH solution added to distil. The distillate was collected into 5 mL of 2% boric acid to which three drops of methyl red and methylene blue indicators were added. The distillate was back titrated against 0.01 M HCl to purplish end point. The cation exchange capacity in biochar was then calculated from the number of moles of HCl consumed in the back titration.

3.2.3 Anion exchange capacity

Five grams of each biochar was weighed into a 100 mL extraction bottle and 50 mL of 1.0 M KNO_3 solution was added. Thereafter, each mixture was shaken on a reciprocating shaker for 30 minutes. The solution was then filtered through a Whatman Number 42 filter paper and excess NO_3^- washed off with methanol. The biochar was leached with 1.0 M KCl and the nitrate ion concentration in the leachate determined by distillation as follows. A 10 mL aliquot of the filtrate was pipetted into a Markham distillation apparatus and 0.2 g of MgO powder was added. Thereafter, 0.2 g of Devarda's alloy and 1 mL of sulphamic acid was added. This was followed by distilling into 5 mL of 2% boric acid to which methyl red and methylene blue indicator mixture had been added in a separate conical flask. The distillate was then titrated against 0.01 M HCl from green to purplish end. The AEC was then calculated from the moles of HCl consumed in the reaction.

3.2.4. Total elemental bases

Total elemental analysis was determined by digesting 0.5 g of biochar with 25 mL of a mixture of concentrated HNO_3 and 60% $HClO_4$ in the ratio of 1:1.5 for 30 minutes. Distilled water was added to the digest, filtered and made up to volume in a 200 mL volumetric flask. Calcium and magnesium contents in the digest were then read on an Atomic Absorption Spectrometer whiles the sodium and potassium was determined using the flame photometer.

3.2.5 Organic carbon

The organic carbon content of the biochar types was determined using the wet combustion method of Walkley and Black (1934). Ten milliliters of 0.167 M potassium dichromate ($K_2Cr_2O_7$) solution and 20 mL of concentrated sulphuric acid (H_2SO_4) were added to a 0.02 g biochar. The flask was then swirled to ensure full contact of the biochar with the solution after which the mixture was allowed to stand for 30 minutes. The unreduced $K_2Cr_2O_7$ remaining in solution after the oxidation of the oxidizable organic carbon in the biochar was titrated with 0.2 M ferrous ammonium sulphate solution after adding 10 mL of orthophosphoric acid and a few drops of barium diphenylamine sulphonate indicator from a dirty brown colour to a bright green end point. A standardization titration of the $K_2Cr_2O_7$ with the ferrous ammonium sulphate was done and the amount of organic carbon calculated by subtracting the number of moles of unreduced $K_2Cr_2O_7$ from the number of moles of $K_2Cr_2O_7$ present in the standardized titration.

3.2.6 Determination of Total Phosphorus.

Total phosphorous was determined by digesting 0.2 g of biochar with 25 mL of a mixture of concentrated HNO_3 and 60% $HClO_4$ in the ratio of 1:1.5. Distilled water was added to the digest, filtered and made up to volume in a 100 mL volumetric flask with distilled water. Phosphorus in the digest was then determined using the Murphy and Riley (1962) method described as follows.

An aliquot of 1 mL of the sample solution was pipetted into a 50 mL volumetric flask and a drop each of P-nitrophenol and ammonium hydroxide were added after which 8 mL of a solution containing concentrated sulphuric acid, ammonium molybdate, potassium antimony tartrate, and ascorbic acid were added. The content was topped up to the 50 mL mark with distilled water. The concentration of phosphorus was then determined on a Philips' UV spectrophotometer at a wavelength of 710 nm and recorded.

3.2.7 Available phosphorus determination

One gramme biochar was weighed into an extraction bottle and 100 mL sodium bicarbonate (pH, 8.5) was added. The bottle was capped and shaken for 30 minutes on a mechanical shaker. The extracts were filtered using a Whatman No. 42 filter paper to obtain clear solution. A 10 mL aliquot was then taken into a test tube and then 1 mL 1.5 M H_2SO_4 added drop-wise to decolourise the solution by settling the organic matter in it. The sample was then left in a refrigerator to cool for few minutes. The extracts in the test tubes were centrifuged, and gently decanted for colour development using the Murphy and Riley method (1962) as described in section 3.3.6 above.

3.2.8 Total nitrogen

Total N of the biochar was determined by the Kjeldahl digestion procedure as outlined by Anderson and Ingram (1993). A 0.02 g of the biochar was weighed into a digestion tube, followed by addition of 5 mL concentrated H_2SO_4. The mixture was heated at low temperature on a digestion block for 30 minutes, and then 2 mL of hydrogen peroxide was added. The heating temperature was maintained until the mixture changed to a permanent colourless solution. The digest was cooled, transferred and made up to volume with the aid of distilled water to the 100 mL mark in a volumetric flask

A 20 mL aliquot was transferred into a tecator distillation flask, and 10 mL of 40% NaOH solution

was added and distilled. The ammonia liberated was condensed and collected in a 10 mL boric acid to which bromocresol green and methyl red solution indicator had been added. The distillate was then back titrated with 0.01 M HCl solution. Similar procedure was adopted for a blank that had no biochar sample to account for traces of N if any, in the reagents and water used. The concentration of N in the biochar was estimated from the number of moles of HCl consumed in the reaction with ammonium borate formed when the ammonia was trapped in boric acid.

3.2.9 Ash content

The ash content of biochar was determined by weighing an empty crucible and recording the weight. Thereafter, a 0.5 g of milled sample of the biochar was weighed into the crucible and placed in a furnace for 1 hour at 600 ^{o}C. The sample was removed and placed in a desiccator to cool. Weight of the ashed sample and crucible was obtained by weighing. Ash content was determined by subtracting the weight of crucible only from the weight of ashed sample and crucible.

3.2.10 X–ray Diffraction

In order to identify the minerals that may be present in the biochar, all the four samples were ground into fine powder in a mortar ensuring that there was no cross contamination. An Empyrean X–ray diffractometer was used for the X–ray analysis. A Cu K–Alpha and Beta radiations were produced using 40 mA and 45 kV power source. The ground samples were mounted on a divergence slit and diffraction patterns of the biochar samples were obtained by scanning the samples at a starting position of 1^{o} per minute between 10^{o} to 60^{o}.

The X-ray diffraction (XRD) patterns were acquired with a computer controlled Panalytical Empyrean X–ray powder diffractometer to determine the type of minerals present.

3.3 Adsorption experiments

A batch adsorption of P on the four biochar types was carried out to ascertain the shaking time for maximum adsorption of the element on the various biochar types, and to determine the effect of pH and concentration of the P on the biochar. These batch experiments were carried out with the ionic strength of the system being kept constant by employing the use of 10 mM NaCl (Nartey *et al.*, 2000).

3.4. Phosphorus solution preparation

To avoid polymerization, a 62 mg/L (2 mM) stock solution of phosphorus was used for the experiment. A stock P solution of the 62 mg/L concentration was prepared from sodium hydrogen phosphate ($NaHPO_4$) Analar grade after drying the chemical in an oven at 70 ^oC. To ensure accuracy, the concentration of the prepared stock solution was cross–checked on a UV spectrophotometer after colour development using the Murphy and Riley (1962) method. It was from this stock solution concentration that other concentrations between 12.4 and 49.6 mg/L (0.4 mM and 1.6 mM) were prepared.

3.5. Sorption experiment

3.5.1 Effect of time on adsorption

Two out of the four-biochar samples namely rice husk and saw dust biochar were used to determine the shaking time for maximum adsorption. A 0.1 g each of the two biochar types was weighed into 60 mL shaking bottles. Various amounts of the stock (62 ppm P) solution were pipetted into 50 mL volumetric flask such that when volumes of 1 M NaCl was added as background solution (for constant ionic strength), the P concentrations in the volumetric flasks were 0.00 mg/L (blank), 0.4 mM (12.4 mg/L), 0.8 mM (24.8 mg/L), 1.2 mM (37.2 mg/L) and 1.6 mM (49.6 mg/L) and the NaCl solution was10 mM NaCl. The P solutions were then added to the shaking bottles containing

biochar and shaken at 200 rpm in a reciprocating shaker at temperature of 22 ± 0.5 ^{0}C at two hour intervals for 24 hours. At the end of each shaking time, the vessels were withdrawn and the mixtures centrifuged at 3000 rpm for 15 minutes to obtain a clear solution for equilibrium P determinations.

The equilibrium P concentrations in the various solutions were determined first by colour development using Murphy and Riley (1962) method. An aliquot of 1mL of the sample solution was pipetted into a 50 mL volumetric flask and a drop each of P-nitrophenol and ammonium hydroxide were added after which 8 mL of a solution containing concentrated sulphuric acid, ammonium molybdate, potassium antimony tartrate, and ascorbic acid were added. The content was topped up to the 50 mL mark with distilled water. The concentration of phosphorus was then read on a Philips' UV spectrophotometer at a wavelength of 710 nm and recorded. The P concentrations on the solid phase were calculated based on the initial and final aqueous concentrations. All the experimental treatments were performed in triplicates and the average values reported. Whenever two measurements showed a difference larger than 5%, the adsorption experiment was repeated for those samples.

3.5.2 Effect of pH on adsorption

Effect of solution pH on phosphate removal by the biochars was studied over a wide initial pH range of 2 to 12 at successive pH increases of 2 pH units (i.e., 2.0, 4.0, 6.0, 8.0 10.0 and 12). Again, a batch sorption experiment was conducted in 60 mL shaking vessels at a temperature of 22 ± 0.5 ^{0}C. About 0.1 g of each biochar sample was weighed into the vessels. Various amounts of the P stock was pipetted into 50 mL volumetric flask and NaCl added so as to attain P concentrations of between 0 and 1.6 mM and NaCl concentration of 10 mM as described in section **3.5.1.** Concurrently, the pHs of the solutions were adjusted to 2, 4, 6, 8, 10 and 12 by adding HCl and/or

NaOH amidst stirring with a magnetic stirrer. The solutions were then made up to volume using de-ionised water which had been pre-adjusted to the various pH of between 2 and 12. The solutions adjusted to their respective pHs were then added to the weighed samples and shaken for six hours as the earlier experiment had found six hours to be the optimum time for maximum adsorption.

At the end of the six hour shaking time, the vessels were removed and the mixtures centrifuged at 3000 rpm for 15 minutes to obtain a clear solutions. The samples were gently decanted and the equilibrium pH immediately determined. The equilibrium P concentrations in the various solutions were determined first by colour development using Murphy and Riley (1962) method as described in section **3.5.1** and then read on a Philips' UV spectrophotometer at a wavelength of 710 nm. The P concentrations on the solid phase were calculated based on the initial and final aqueous concentrations. All the experimental treatments were performed in triplicates and the average values are reported. Whenever two measurements showed a difference larger than 5%, the adsorption experiment was repeated for those samples.

Calcium and Mg that may have been released into solution during the adsorption experiment were determined using an Atomic Absorption Spectrometer.

3.6 Quantity adsorbed

The amount of P adsorbed onto the various biochars were calculated using the equation:

$$\boldsymbol{qt = \frac{(C_o - C_t)V}{m}} \qquad (\boldsymbol{Eqn.3.1})$$

Where qt (mg/kg) is the amount of P per mass unit of biochar at time t, C_0 and C_t (mg/L) are the initial and at equilibrium concentration of P, respectively, V is the volume of the solution (L), and m is the mass of adsorbent (g).

3.7 Sorption Isotherms

A plot of quantity of P adsorbed (mg/kg) against time (hours) was drawn to analyse the effect of time on the adsorption. In addition, quantity of P adsorbed per unit mass of biochar was plotted against the equilibrium P concentration to determine the sorption maxima for the four biochar types as well as P adsorbed per unit mass against equilibrium pH to determine the optimum pH for maximum adsorption.

3.8 Data analyses

The quantity of P adsorbed at the different time internals as well at the different pHs were subjected to analysis of variance (ANOVA) using Genstat 9 to establish whether there were differences in the biochar type with respect to P sorption from aqueous solution.

CHAPTER FOUR

RESULTS

4.1 Characterization of biochar

4.1.1 Physico-chemical properties

Some physical and chemical properties of the four biochar types used for the adsorption studies are shown in Table 4.1. Ash content of the biochars was in the range 2 to 42% and varied with the biochar types as noted by Yuan and Xu (2012) who observed similar variation in ash content of different biochar types. The ash content of the biochar types was in the order rice husk > cocoa pod > saw dust > rice straw with values being respectively, 42%, 34% 4% and 2%.

The pH in water was near neutral for the sawdust biochar (SD) with value of 7.4 and slightly alkaline (7.7) for the rice husk. The near neutral to slightly alkaline nature of biochar for rice husk and sawdust (7.4-7.7) is typical with biochar prepared from these plant materials and is consistent with results obtained by Eduah (2012) and Antwi-Bosiako (2012) for sawdust and rice husk biochars. The rice straw (RS) and cocoa pod (CP) biochar were strongly alkaline with values of 9.4 and 10.4, respectively. The pH in 0.01 M $CaCl_2$ did not show any marked difference from that in water with values of 10.7, 7.6, 9.4 and 7.4 for CP, RH, RS and SD, respectively. Strikingly, the electrical conductivity (EC) measured was highest in the cocoa pod biochar with a value of 1.8 dSm^{-1}. The other three biochar types had very low EC values of 0.42 dSm^{-1} for the rice straw, 0.03 dSm^{-1} for the rice husk and 0.04 dSm^{-1} for the saw dust.

Table 4. 1: Some physico-chemical properties of the four biochar types.

Biochar type	Ash (%)	pH H_2O	pH $CaCl_2$	Avail. P mg/kg	EC dS/m	OC ..... g/kg.....	TN	TP mg/kg
CP	34.0	10.4	10.7	3987.7	1.8	256.0	3.5	4700
RH	42.0	7.4	7.6	531	0.03	290.0	1.4	1100
RS	2.0	9.4	9.3	1193.3	0.42	490.0	2.1	3000
SD	4.0	7.7	7.4	249	0.04	480.0	2.1	800

CP = Cocoa pod biochar

RH = Rice husk biochar

RS = Rice straw biochar

SD = Sawdust biochar

Table 4. 2: Total and exchangeable bases, CEC, and AEC of the four biochar types.

	Total Bases				Exchangeable bases				Surface charges	
Biochar type	Na	K	Ca	Mg	Na	K	Ca	Mg	CEC	AEC
	……%.....				……cmol/kg……					
CP	13.8	2.01	0.48	0.50	43.6	12.5	4.7	16.89	81.61	38.98
RH	1.90	0.09	0.26	0.09	1.90	4.1	0.97	0.90	38.89	28.12
RS	6.30	0.97	0.48	0.24	10.5	7.4	9.99	6.21	50.56	37.89
SD	1.25	0.13	0.67	0.15	8.70	4.08	10.48	1.29	46.67	28.91

CP = Cocoa pod biochar

RH = Rice husk biochar

RS = Rice straw biochar

SD = Sawdust biochar

The organic carbon (O.C) content varied with biochar type. The rice straw and the saw dust had the highest O.C contents of between 480 and 490 g/kg with the rice husk biochar recording an organic carbon content of 290 g/kg. The cocoa pod had the least organic carbon content of 256 g/kg. Total N of the four biochar types were expectedly very low and less than 4 g/kg. The highest total N content was found in the cocoa pod biochar (3.5 g/kg) with the rice straw and saw dust recording similar values of 2.1 g/kg. The lowest total N content of 1.4 g/kg was observed in the rice husk biochar. Again, the total and available phosphorus content of cocoa pod and rice straw biochar was higher than the rice husk and sawdust with the cocoa pod biochar recording total and available phosphorus of 4700 mg/kg and 3989.7 mg/kg respectively, which was the highest among the four-biochar types. Rice straw biochar had total phosphorus of 3300 mg/kg with 1193.3 mg/kg available phosphorus whiles the rice husk had a total phosphorus of 1100 mg/kg and 531 mg/kg available phosphorus. The sawdust recorded the lowest total phosphorus of 800 mg/kg and an available phosphorus of 249 mg/kg.

The total and exchangeable bases are presented in Table 4.2. From the table, it is seen that the total percentage bases in the biochar samples were highest in the cocoa pod biochar type. The % Na in the CP was 13.8% and more than twice the value recorded in the rice straw biochar type (6.3%). The rice husk and the saw dust biochar types had respectively, 1.9 and 1.25% total Na. The %K in the CP was highest (2.01%) and again more than twice the K content in the rice straw (0.97%). The rice husk and the saw dust had the least values of K ranging between 0.09 and 0.13%. Total Ca of 0.67% was highest in the SD with the CP and RS having total Ca content of 0.48%. The least total Ca content of 0.26% was observed in the RS biochar. The total Mg content of 0.59% was highest in the CP followed by the RS. The RS element accounted for only 0.24% of total

elements. The RH and SD had the lowest total Mg contents accounting for between 0.09% and 0.15% of the total elements analysed.

The concentration of exchangeable Na was expectedly the highest of all the bases particularly in the CP, RS and the SD biochar samples. The trend of exchangeable Na followed that of the total sodium and was in the order of CP > RS > SD > RH. The highest Na concentration of 43.6 cmol/kg in the CP was more than four times that in the RS (10.5 cmol/kg). The exchangeable K in the biochar samples reflected the pattern of total K contents and was in the order of CP > RS > SD ~ RH. Exchangeable Ca of 10.28 cmol/kg was highest in the SD with the lowest concentration of the nutrient (0.97 cmol/kg) being found in the RH. Even though total Ca contents were similar in the CP and the RS, the exchangeable form of the nutrient was almost 2.1 times higher in the RS than in the CP. The exchangeable Mg concentration of 16.89 cmol/kg, (the highest) was recorded in the CP. This concentration of the nutrient was almost 2.7 times that found in the RS and approximately 18.8 times that found in RH. The SD had an exchangeable Mg content of 1.29 cmol/kg.

The cocoa pod biochar had a very high cation exchange capacity of 81.67 cmol/kg. The CP's CEC was 42.78 cmol/kg, 35 cmol/kg and 31.11 cmol/kg respectively, higher than CECs recorded in the RH, SD and RS. Anion exchange capacity which is a measure of the amount of anions that could be adsorbed was similar for the biochar from the cocoa pod (39.98 cmol/kg) and rice straw (37.89 cmol/kg). The average AEC of these two biochar types was approximately 10 cmol/kg more than the average AEC of biochars from the rice husk and sawdust.

4.1.2 Mineralogical composition of the biochar types

The x-ray diffractograms of the various biochar types are presented in figures 4.1 a, b, c and d and the mineral type present in the four biochar types have been tabulated in Table 4.3. From the diffractograms and the table, it is seen that the most abundant mineral present in all the four biochar types is silica. The cocoa pod biochar in addition to having large quantities of silica also had appreciable amounts of $KHCO_3$, $AlFeO_3$ and small quantities of $MgCO_3$, MgO and $KHCO_3$.

Though the feedstock for RH production came from the same rice plant as the RS, apart from silica, the two biochar types were completely different in mineralogical composition. The RS had in addition to silica, large quantities of calcite ($CaCO_3$), siloxene (Si_2OH_2), and KCl and very small quantities of calcium differate ($CaFe_2O_4$), and MgO whereas the RH had in addition to silica only $Mg(OH)_2$. The SD had large quantities of calcite ($CaCO_3$), silica (SiO_2) and nitrated graphite. There were small quantities of iron oxide (Fe_2O_3), iron magnesium oxide (Fe_2MgO_4), magnesium silicate (Mg_2SiO_4) and magnesium oxide (MgO).

4.2 Sorption isotherms

4.2.1 Effect of time on adsorption

The effect of time on adsorption for the rice husk and saw dust biochars are presented in Fig 4.2. From the figure it is seen that adsorption of P on the two biochar types used for the experiment increased with time up to six hours. Adsorption of phosphorus onto the biochar was rapid within first two hours during which period the RH adsorbed approximately 6900 mg/kg P with the SD adsorbing 6952 mg/kg P.

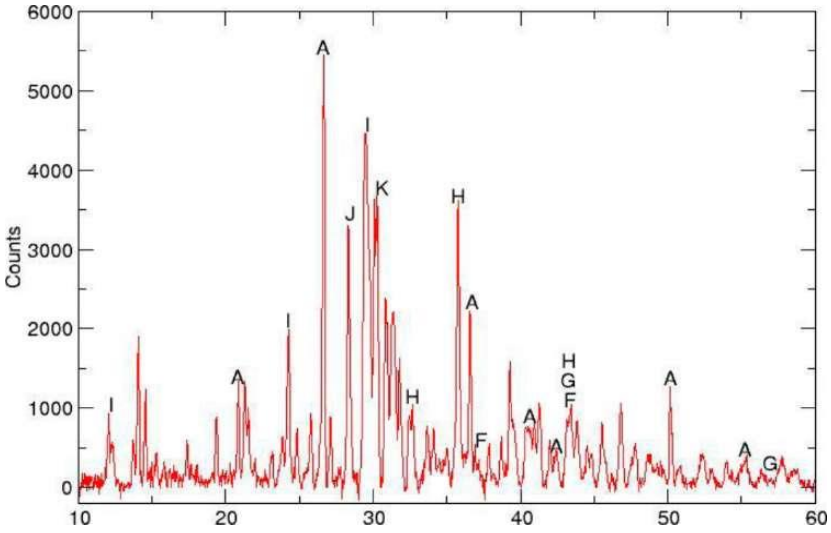

Figure 4.1 a: X–ray diffractogram of cocoa pod biochar.

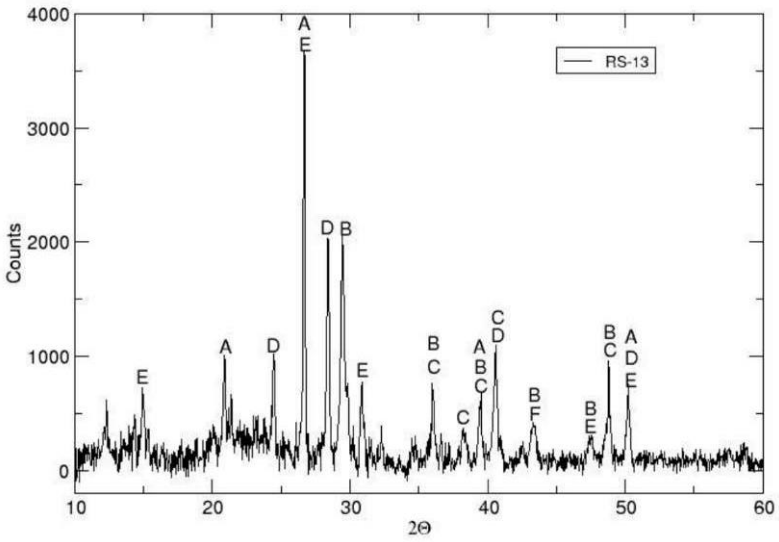

Figure 4.1b: X–ray diffractogram of rice straw biochar.

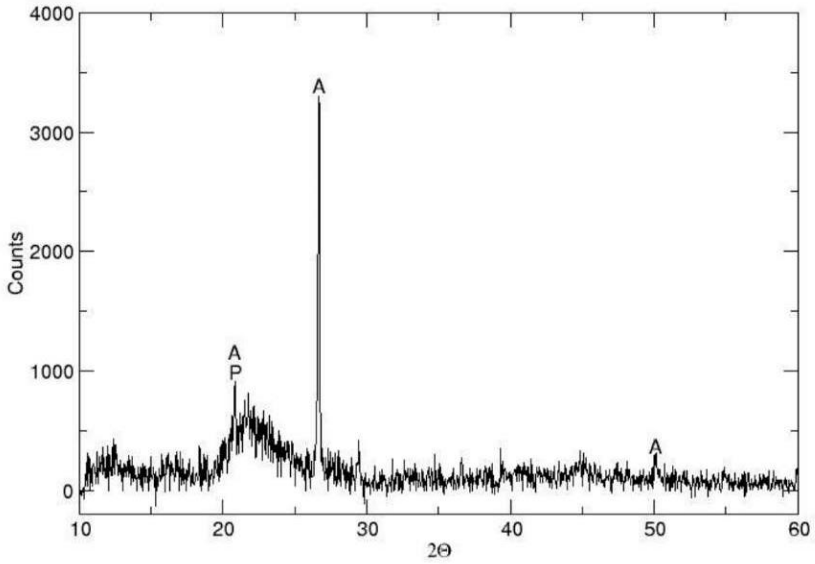

Figure 4.1c: X–ray diffractogram of rice husk biochar.

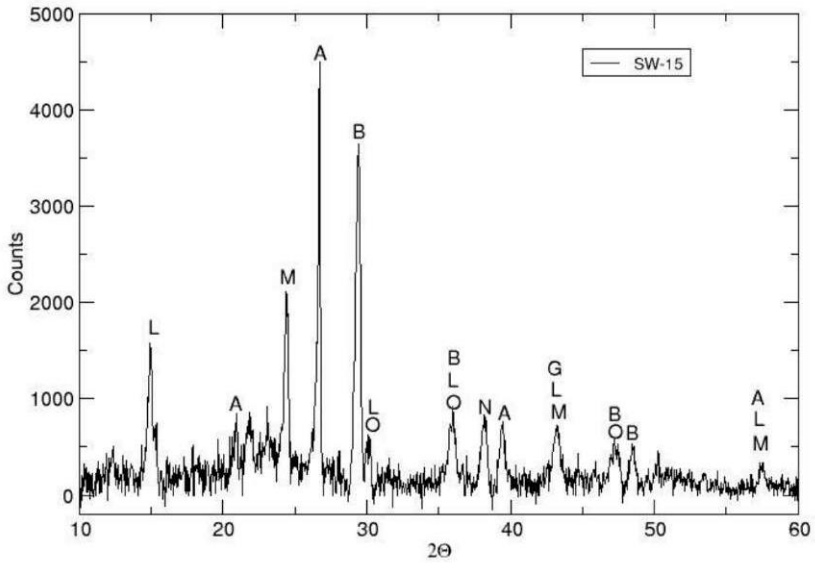

Figure 4.1d: X–ray diffractogram of sawdust biochar.

Table 4. 3: Mineralogical composition of the four biochar types*

Mineral	Key	Biochar type			
		CP	**RH**	**RS**	**SD**
Silicon Oxide (SiO_2)	A	A	A	A	A
Calcium Carbonate ($CaCO_3$)	B			B	B
Calcium Differate Oxide ($CaFe_2O_4$)	C			c	
Potassium Chloride (KCl)	D			D	
Siloxene (H_2OSi_2)	E			E	
Periclase (MgO)	F	F		f	
Magnesium Oxide (MgO)	G	G			g
Magnesium Carbonate ($MgCO_3$)	H	h			
Potassium Hydrogen Carbonate ($KHCO_3$)	I	I			
Aluminium Iron Oxide ($AlFeO_3$)	J	J			
Iron Oxide Hydroxide (K)	K	K			
Iron oxide (Fe_2O_3)	L				
Graphite, Nitrated		M			
Magnesium Silicate (Mg_2SiO_4)	N				
Iron Magnesium Oxide ($FeMgO_4$)	O				
Magnesium Hydroxide ($Mg[OH]_2$)	P		p		
Potassium Magnesium Carbonate ($KMgCO_3$)	Q	q			

*Lower case = minor component.

Uppercase = Major component

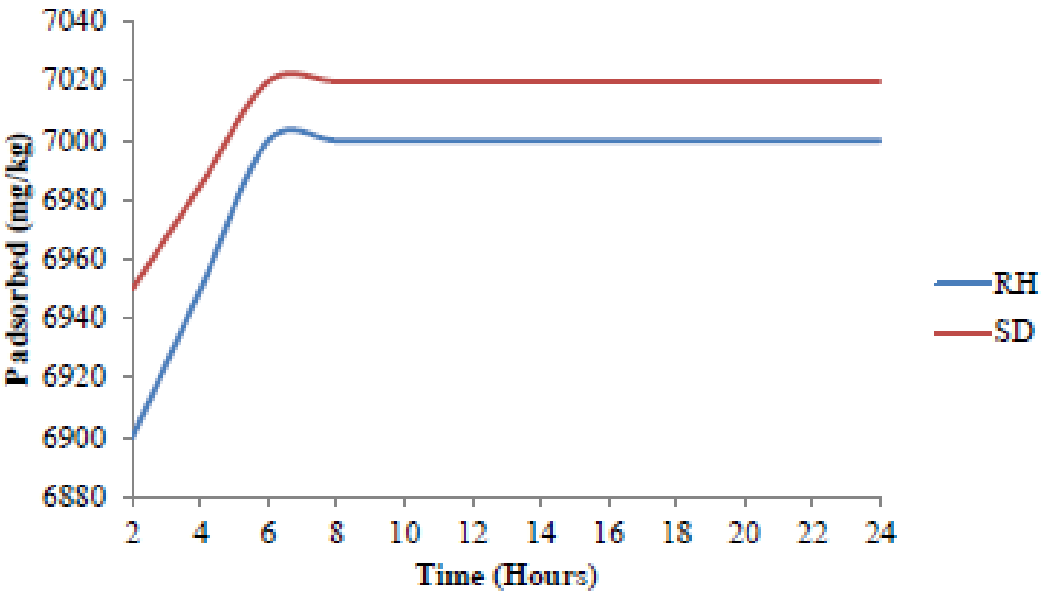

Figure 4.2: Effect of shaking time on phosphorus adsorption.

Further shaking up to six hours increased P adsorption on the RH by only 105 mg/kg whilst that on the SD was increased by a paltry 73 mg/kg. Statistical analysis showed that there were no significant differences (5%) among quantities adsorbed between 2 hours and 6 hours. Amount of P adsorbed, irrespective of the biochar type after six hours of shaking remained the same.

4.2.2 Effect of pH and concentration on Adsorption

The two most common statistical modelling methods employed in the study of adsorption processes are the Langmuir and the Freundlich equations. The adsorption results conformed to the Langmuir equation with R^2 values ranging between 0.98 and 0.99 and this is in agreement with the findings of Yao *et al.* (2011b).

Adsorption isotherms of phosphorus onto the four biochars, rice husk, and rice straw, cocoa pod and sawdust at different concentrations of phosphorus and initial pHs of between 2 and 12 are shown in Figs 4.3 a, b, c and d. The adsorption of phosphate onto the various biochars depended on initial solution pH with maximum adsorption occurring at initial pH 4 for rice husk, rice straw and sawdust biochar. Strikingly, the CP with the highest pH in both H_2O and $CaCl_2$ had its highest adsorption at initial pH 2 and not 4 (Fig. 4.3 d). Generally, amount of P adsorbed at any given initial pH and initial concentration was in the order of SD ~ RH > RS > CP. At initial pH 4, the SD with least pH in both water (7.7) and salt (7.4) adsorbed between 3400 mg/kg and 6900 mg/kg P. The RH with similar pH in both water (7.6) and salt (7.4) as the SD also adsorbed between 3300 mg/kg and approximately 7000 mg/kg P. The RS with a strongly alkaline regime of pH of between 9.3 and 9.4 had adsorption between 3300 mg/kg and about 6100 mg/kg. The CP with an inherent pH of between10.4 and 10.7 had the highest adsorption of P at initial pH 2 and the concentration adsorbed was between approximately 2800 mg/kg P and 5800 mg/kg P.

The isotherms indicate that there was an optimum equilibrium pH for maximum adsorption which was dependent on biochar type and initial P concentration (Fig. 4.4 a-d.). At equilibrium pH 2.2 and 2.3, the RH and the SD adsorbed 2250 mg/kg P when initial concentration of P added was 12.4 mg/L or 0.4 mM. At respective equilibrium pHs of 6.2 and 6.6 for the RH and the SD and at the same P concentration of 0.4 mM, maximum P of about 3400 mg/kg was adsorbed. Increasing equilibrium pH beyond 6.2 and 6.6, respectively for the RH and SD to 11.8 led to decreases in P adsorption to values lower than amount adsorbed at equilibrium pH 2.3.

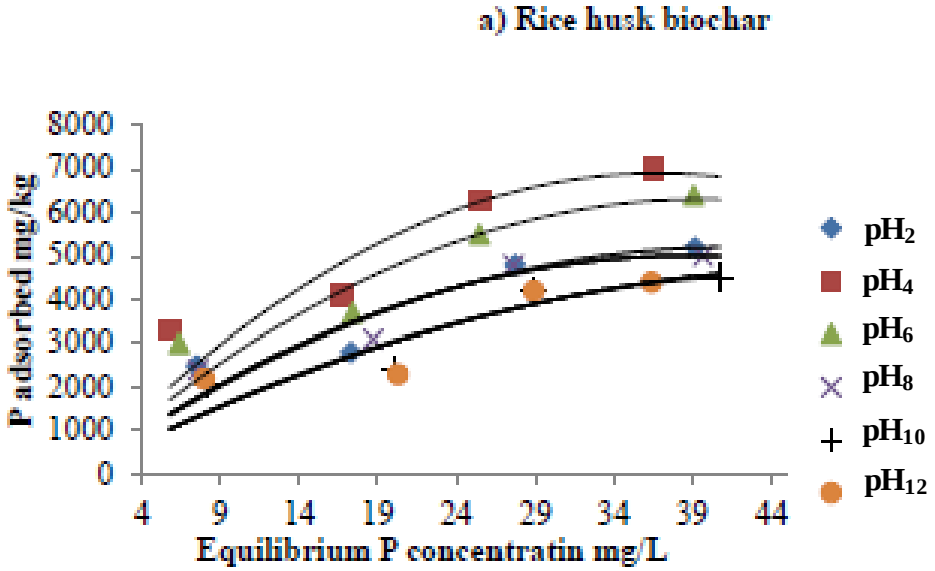

Figure 4.3a: Isotherms of Phosphorus on rice husk biochar.

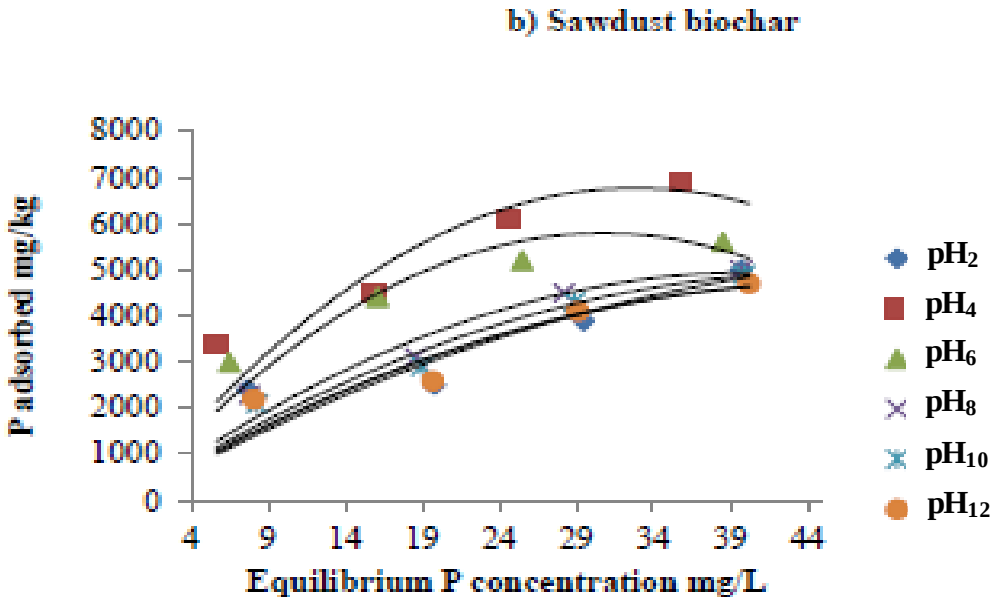

Figure 4.3b: Isotherms of Phosphorus on sawdust biochar.

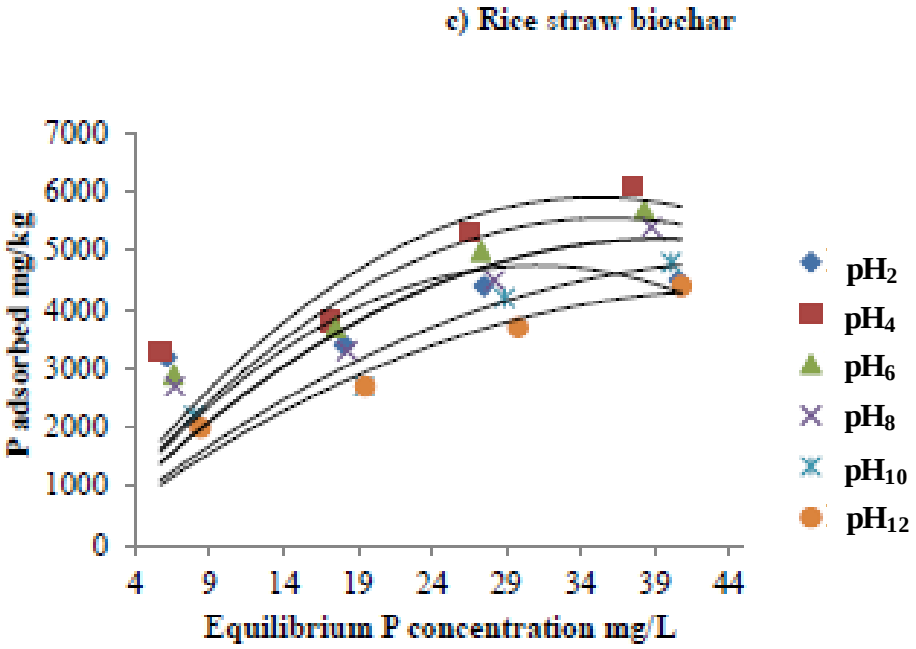

Figure 4.3c: Isotherms of Phosphorus on rice straw biochar.

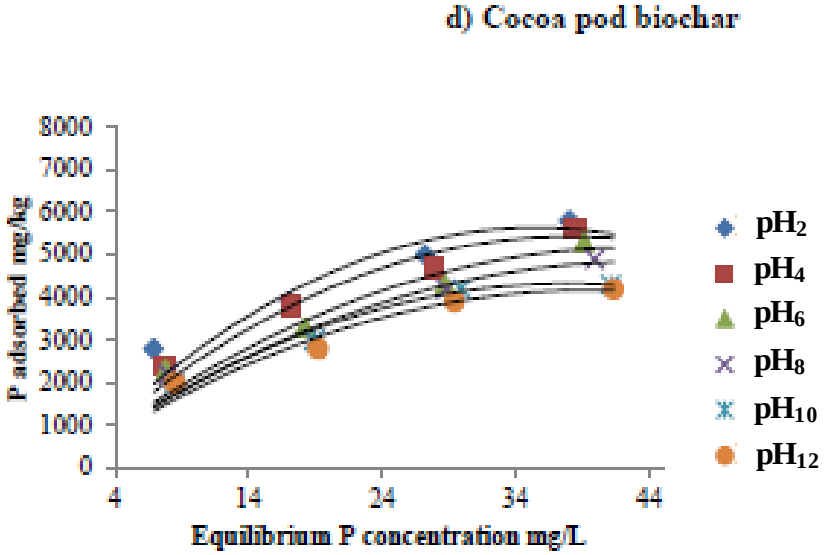

Figure 4.3d: Isotherms of Phosphorus on Cocoa pod biochar.

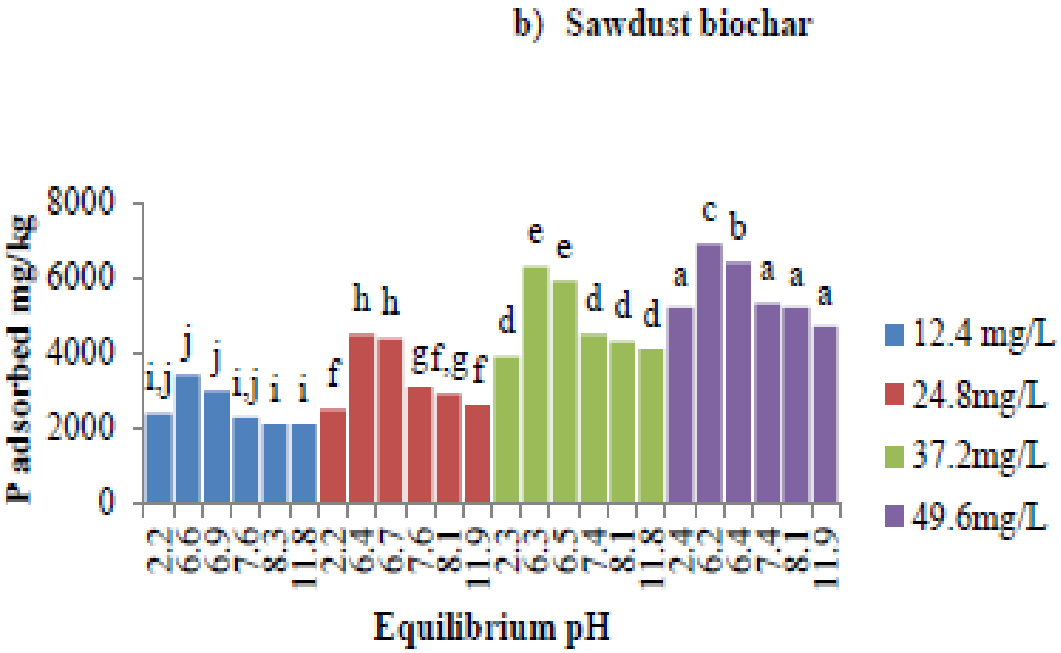

Figure 4.4a: Effect of equilibrium pH on P adsorption on rice husk biochar.

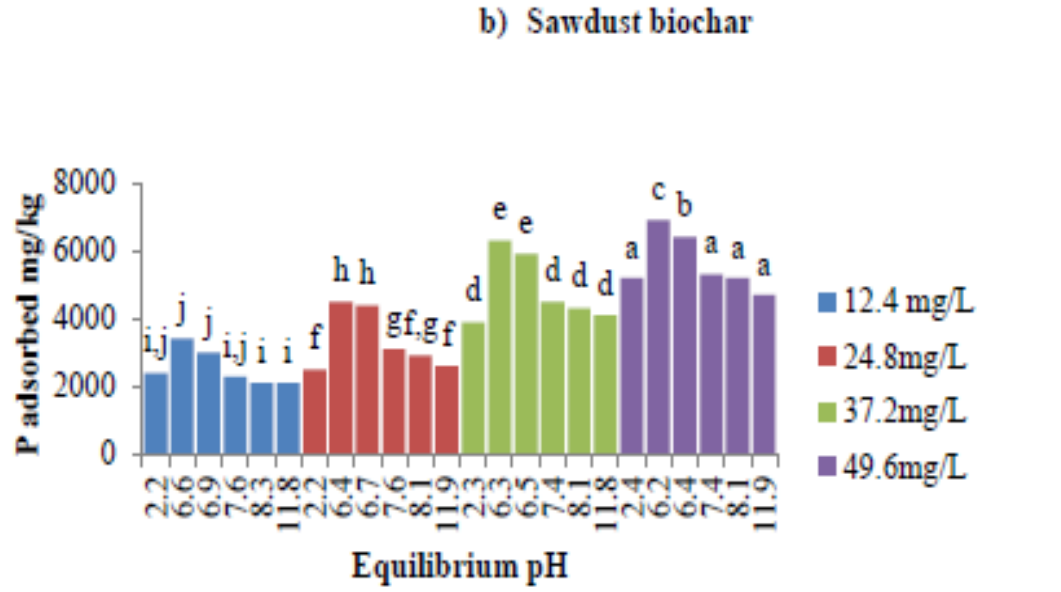

Figure 4.4b: Effect of equilibrium pH on P adsorption on sawdust biochar.

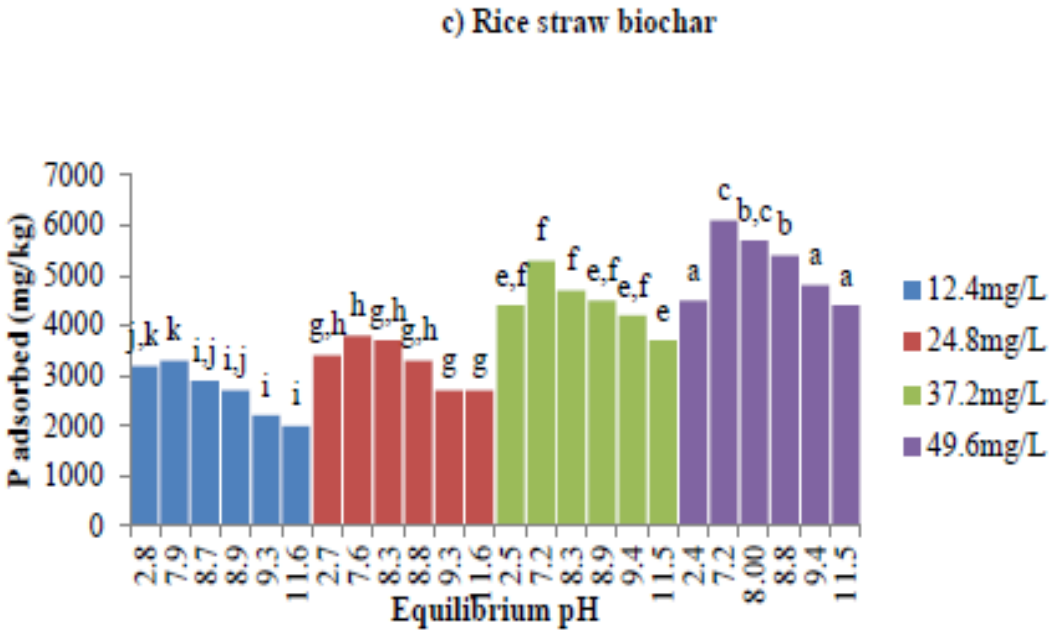

Figure 4.4c: Effect of equilibrium pH on P adsorption on rice straw biochar.

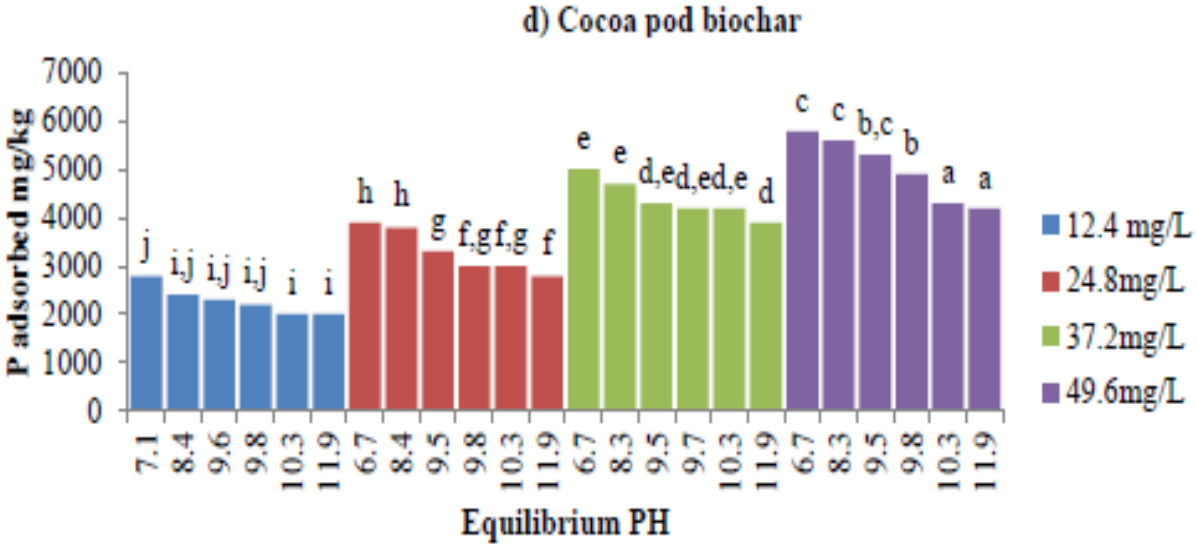

Figure 4.4d: Effect of equilibrium pH on P adsorption on cocoa pod biochar.

Similar trends were observed for the RH and SD at increasing initial P concentration of 24.8 mg/L (0.8 mM), 37.2 mg/L (1.2 mM) and 1.6 mM. Maximum P adsorption at initial concentration of 24.8 mg/L, 37.2 mg/L and 49.6 mg/L occurred at respective equilibrium pHs of 6.1, and 5.7 for the RH whilst that of the SD, equilibrium pHs for maximum adsorption were at 6.4, 6.3 and 6.2, respectively.

At equilibrium pH 2.8 and at initial P concentration of 12.4 ppm, the rice straw biochar adsorbed approximately 3200 mg P/ kg biochar. When equilibrium pH increased by 5.1 pH units, increase in P adsorbed was marginal. Increasing equilibrium pH further to 11.6 decreased P adsorption to approximately, 2000 mg P / kg biochar. This decrease at equilibrium pH 11.6 was about a 1000 mg P/kg biochar less than that at equilibrium pHs 2.8 and 7.9. Increasing initial P concentrations elevated P adsorption with maximum adsorption occurring at equilibrium pH 7.6, 7.2 and 7.2, respectively for initial P concentrations 24.8 mg/L, 37.2 mg/L and 49.6 mg/L. Increasing equilibrium pH above the optimum led to decreases in the concentration of P adsorbed.

It is worth noting that for the rice straw at lower initial concentration of 12.4 mg/L there was no statistical difference in P adsorbed at equilibrium pH 2.8 and 7.9 and at 2.7 and 7.6 for initial concentration 24.8 mg/L. However, at higher concentrations of 37.2 ppm, amount adsorbed was statistically significant with 1000 mg/kg P more adsorbed when pH increased from 2.5 to 7.2. A similar trend was observed at 49.6 initial P concentrations, where almost 1500 mg/kg more P was adsorbed when equilibrium pH increased from 2.4 to 7.2.

The cocoa pod (very high pH of 10.4) expectedly after equilibration with the P solution at the various initial concentrations and at initial pH 2, had its equilibrium pH ranging between 6.7 and 7.1. The equilibrium pH was highest (7.1) at initial P concentration of 12.4 ppm. Increasing

equilibrium pH at all the various initial concentrations of P led to decreases in adsorption with the least adsorption occurring at equilibrium pH 11.9.

Generally, increasing equilibrium pH from 2.2 to about 6.9 for the RH, SD and RS resulted in increasing P adsorption (Fig 4.4a-d) beyond which adsorption decreased

4.2.3 Effect of pH on maximum phosphorus adsorption

The overall maximum adsorption occurred on the rice husk biochar at an equilibrium pH of 5.7 with a maximum phosphorus adsorption of 7010 mg/kg. This was followed by the sawdust biochar with maximum adsorption of 6940 mg/kg occurring at an equilibrium pH of 6.2. The rice straw biochar was next with a maximum adsorption of 6100 mg/kg, which occurred at an equilibrium pH of 7.2. The cocoa pod biochar had the lowest adsorption of 5800 mg/kg that occurred at an equilibrium pH of 6.7. Adsorption on the various types of biochars increased in the order of rice husk biochar > saw dust biochar > rice straw biochar > cocoa pod biochar. Statistical analysis at 95% confidence level revealed that there was no significant difference between adsorption at pH 6.7 and 7.2. There was also no significant difference between adsorption at pH 5.7 and 6.2. However, there were differences in adsorption at pH 5.7 - 6.2 and pH 6.7 - 7.2.

4.2.4 Phosphorus sorption capacity (Pmax) for the various biochars

To estimate the Langmuir sorption maximum which measures the maximum amount of phosphorus (P max) that can be sorbed on the adsorbent (biochars) and the binding energies for the various biochar types, the equilibrium concentration of P (Ce) as a fraction of quantity of P adsorbed (qe) per unit biochar was plotted against the equilibrium concentration for the various biochar types. Linear and curvilinear models were fitted to the graphs (Figure 4.5) from which the q max and the binding energies were calculated. The goodness of fit of the model was ascertained

by looking at the R^2 values. All the plots were highly significant with R^2 values range from 0.98 to 0.99 indicating apparent high conformity of the adsorption data to the Langmuir model.

Table 4.4 shows the calculated P max and the accompanying binding energies for all the biochar types. The results indicated that the rice husk biochar and the sawdust biochar had the same sorption capacity and the highest sorption capacity with Pmax values of 7300 mg/kg, which occurred between equilibrium pH of 5.7 and 6.2. The rice straw biochar with a Pmax of 6300 mg/kg occurred at equilibrium pH of 7.2 and this is 1000 mg/kg more than the P max for the cocoa pod biochar that occurred at equilibrium pH of 6.7. The binding energies, b, (0.2 L/mg) for rice husk, sawdust, and rice straw biochar types were the same whiles the cocoa pod biochar had a lower energy of 0.18 L/mg.

4.2.5 Change in pH with adsorption

The pH of the blank run (0 concentration of P) was considered the initial pH of the biochar samples mixed with phosphorus at various concentrations and pH. To ascertain whether the change in pH was a reflection of adsorption, concentration of P adsorbed was plotted against change in pH and the results are shown in Figure 4.6 a-d. From the figures, there was generally no change in solution pH with increasing adsorption in the rice RH since most of the changes in pH were below 0.5 pH units (Nartey *et al.*, 2001). It is worthy of note that, the SD which had the highest adsorption, maximum adsorption coincided with a 1.2 decrease in pH after adsorption at initial pH 4 and 6. The RS and the CP did not generally experience changes in pH with increasing adsorption since most of the ΔpHs were below 0.5 pH units.

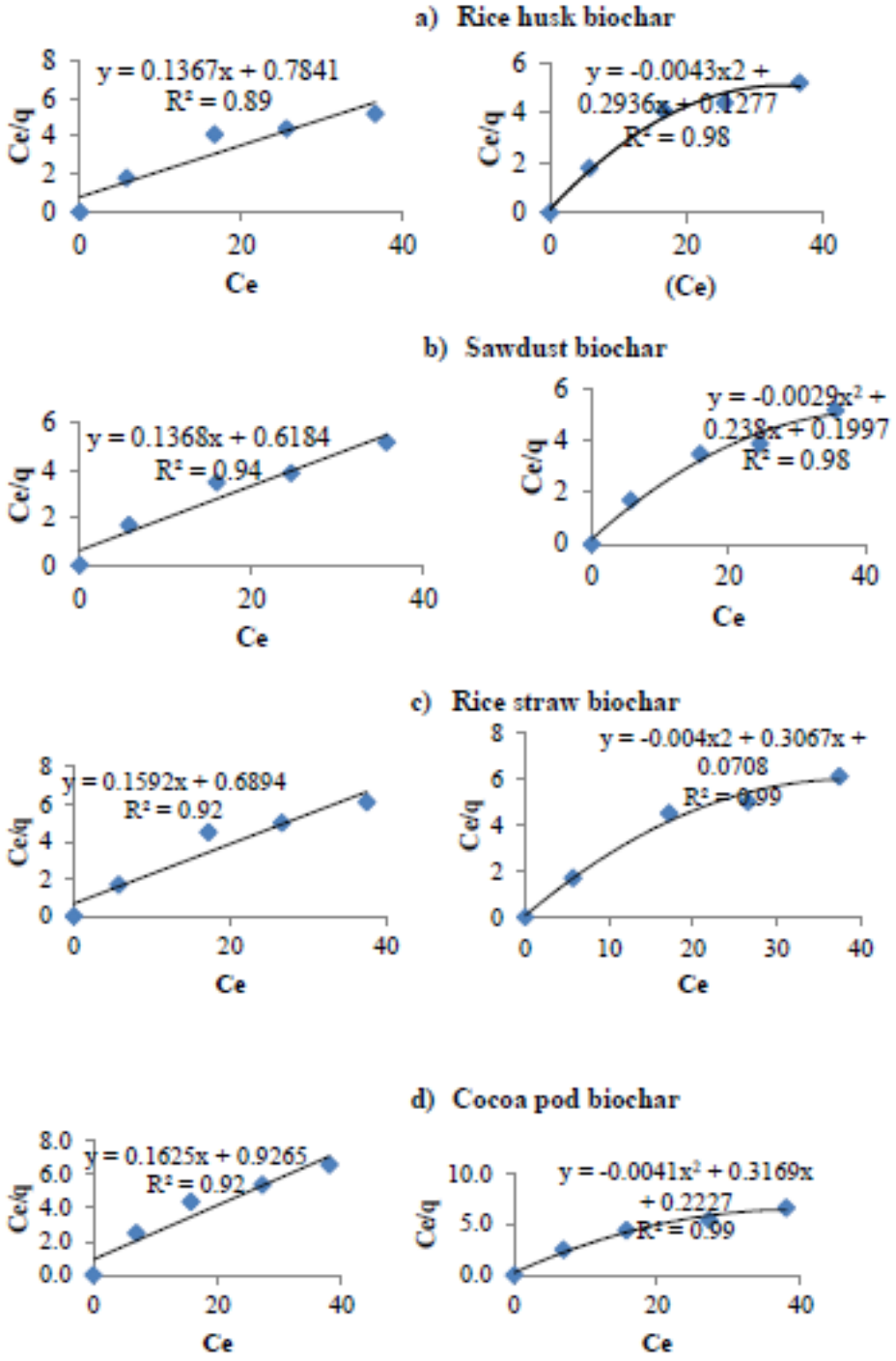

Figure 4.5: Linear and curvilinear fitting graphs of the four biochar types for Pmax.

Table 4.4: maximum phosphorus sorption capacity and binding energies from Langmuir model.

Biochar types	**Pmax*** **(mg/kg)**	**b+** **(L/mg)**	**R^2**
Cocoa pod	6200	0.18	0.99
Rice straw	6300	0.20	0.99
Rice husk	7300	0.20	0.98
Sawdust	7300	0.20	0.98

*Pmax = maximum phosphorous sorption capacity

+ b = binding energy

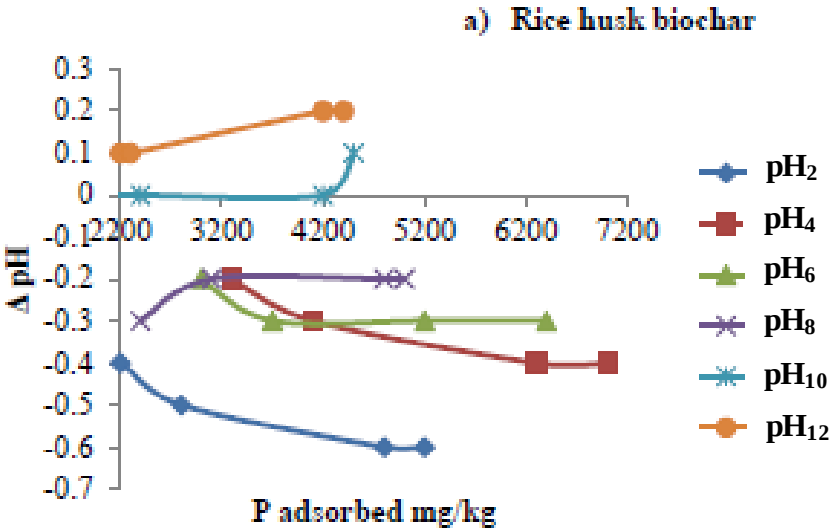

Figure 4.6a: Change in equilibrium pH with P adsorption on the rice husk biochar.

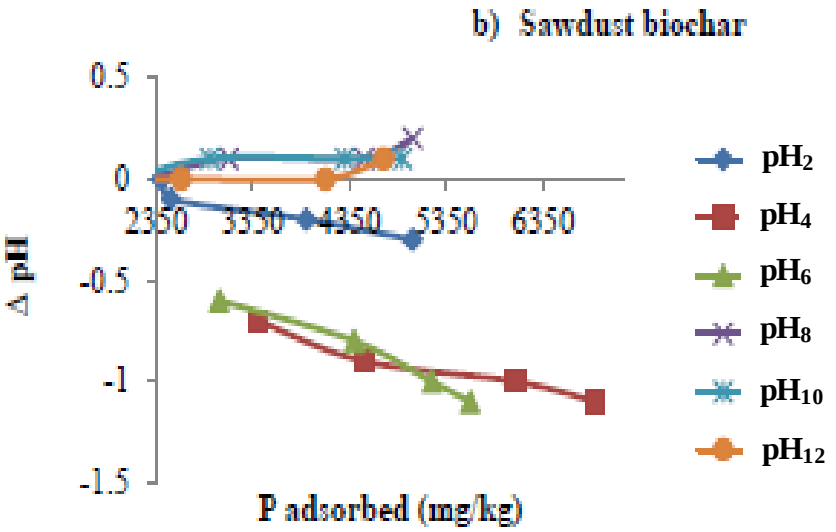

Figure 4.6b: Change in equilibrium pH with P adsorption on the sawdust biochar.

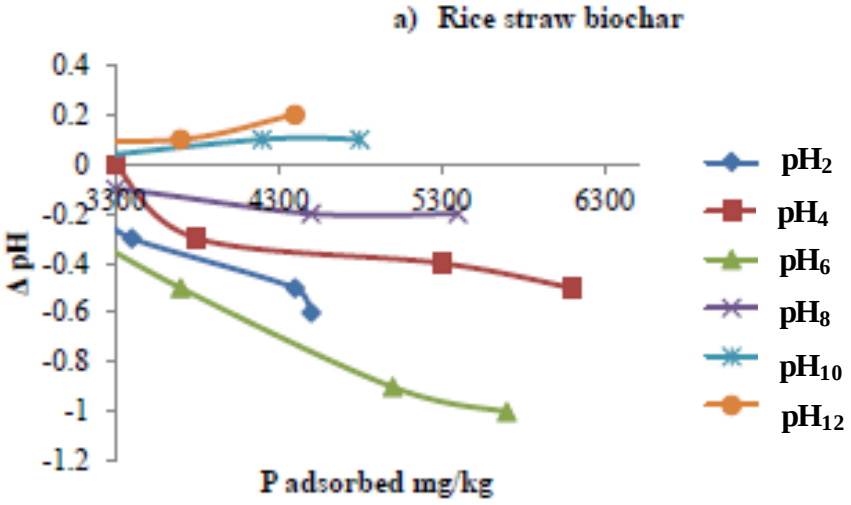

Figure 4.6c: Change in equilibrium pH with P adsorption on the rice straw biochar.

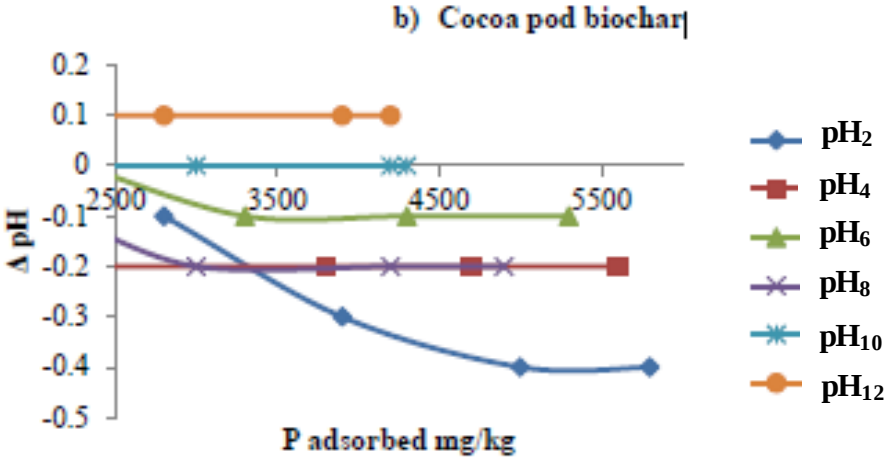

Figure 4.6d: Change in equilibrium pH with P adsorption on the cocoa pod biochar.

4.2.6 Ca and Mg release with adsorption

To ascertain whether the release of Ca and Mg was as a result of adsorption, concentrations of the two elements in equilibrium solutions were plotted against P adsorbed (Figs 4.7 a and b). The Ca released into solution was between 0.056 and 0.072 mg/L for RH. However, this level of Ca released did not reflect adsorption with a coefficient of determination was 0.0323. The amount of Mg released (0.0024 – 0.0192 mg/L) into solution by the rice husk biochar reflected adsorption of phosphate onto the biochar as R^2 value was 0.91* indicating a strong relationship between Mg released and P adsorbed. The highest release of Mg (0.0192 cmol/kg) occurred at equilibrium pH 5.7 which coincided with the highest P adsorption. Similarly, 0.08 – 0.16 mg/L of Ca and 0.0048 – 0.0169 mg/L of Mg were released into solution for the sawdust biochar. The amounts of Ca and Mg released were positively correlated with the P adsorption with R^2 values of 0.85* and 0.89*, respectively. The high R^2 values revealed a strong relationship between amounts of P adsorbed with Ca and Mg released.

Rice straw biochar released between 0.004 – 0.08 mg/L of Ca and 0.072 – 0.0168 mg/L of Mg into solution. However, both the Ca and Mg released had no relationship with P adsorbed as the R2 value of 0.76 was not significant at 5% probability level. On the other hand, Mg released did not reflect the adsorption of phosphate onto the rice straw biochar.

Cocoa pod biochar released 0.076 mg/L of Ca and 0.0168 mg/L Mg, which was the same at all pHs. The amount of Ca and Mg released into solution by the CP biochar did not reflect the adsorption of phosphate onto the material.

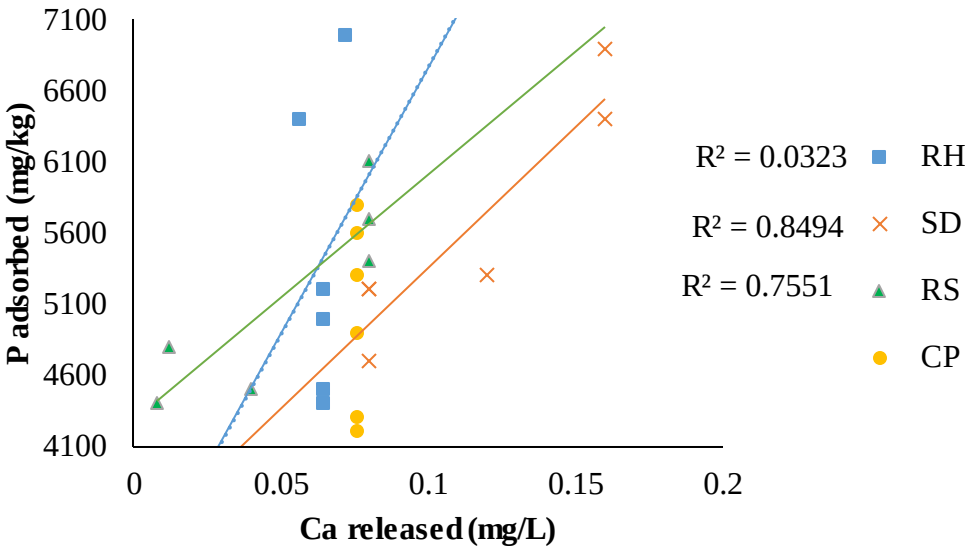

Fig 4.7a: Relationship between P adsorbed and Ca released.

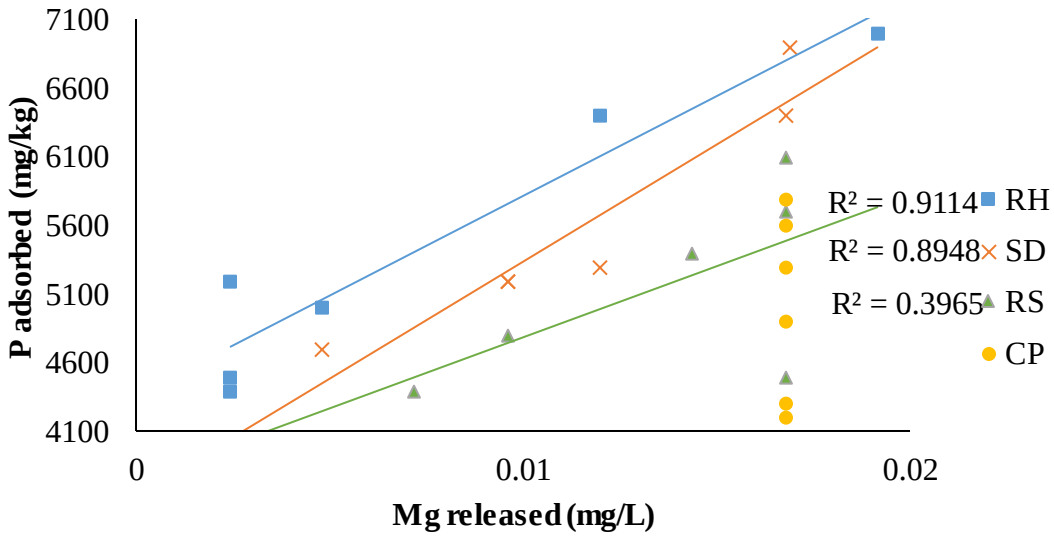

Fig 4.7b: Relationship between P adsorbed and Mg released.

CHAPTER FIVE

DISCUSSION

5.1 Characterization of biochar

The comparatively higher ash contents in the RH (42%) and CP (34%) is an indication that the feed stock i.e. cocoa pod and rice husk from which the two biochar types were prepared are more prone to combustion. The feedstock for the SD is mainly woody material and it is expected that this material and the rice straw would be more lignified than the cocoa pod and rice husk and hence more resistant to combustion. For higher yield per unit mass of RH and CP, therefore, lower temperatures than the 450°C used in this study will be better.

The higher pH values (>7) of the four biochar types are due to pyrolysis (Struebel, 2011). At pyrolysis temperatures between 300 °C to 600 °C, organic acids and phenolic substances are released during the cracking of hemicellulose and cellulose. These acids then combine with basic cations in the feedstock to form alkali salts with a concomitant increase in pH of the biochar (Streubel, 2011; Shinogi and Kanri, 2003). It is evident that the type of feedstock has accounted for differences in pH of the four biochar types. The concentrations of both total and exchangeable bases particularly K, Ca and Mg are highest in the CP followed by the RS and this is reflected in the strongly alkaline pH of these two biochar types with the CP having the higher pH. The strongly alkaline pH (10.4) in the CP is further corroborated by the presence of appreciable quantities of $KHCO_3$, and $MgCO_3$ and small quantities of MgO which are all liming materials. The RS also has large amounts of calcite and periclase which may, in part, have influenced the material's strongly alkaline pH.

Electrical conductivity (EC) is a measure of the ability of the biochar to conduct electrical current and is used to estimate salinity (Essay, 2013; Doerge, 1999). The EC measurements also have the potential for estimating variation in physical properties such as moisture content and porosity. Presence of charged species (such as Na^+, K^+, Ca^{2+}, Mg^{2+},) especially high exchangeable Na enhances the electrical conductivity of the material (Essay, 2013). The high total and exchangeable Na in the CP may account for the material's high EC.

According to Doerge (1999), high EC of biochar connotes greater porosity which may imply that cocoa pod biochar may have higher porosity than the other biochar materials. Though the EC of the CP is not up to the critical level (4 dS/m), its continuous application to soils, particularly those high in Na content may lead to the destruction of the structure of those soils. The low EC of the other biochar types is as a result of their low total levels exchangeable Na^+. These low EC values imply these biochar types would be better suited for P enrichment of soils with minimal Na threat should they be amended to soils.

In all, cocoa pod biochar had the highest nutrient concentrations with respect to total N and exchangeable bases with the exception of Ca. High concentrations of these nutrients in the cocoa pod biochar coupled with its high pH and the abundance of liming potential make it a suitable material to be used as soil amendment in highly acidic Oxisols such as the Ankasa and Boi series in the Western Region of Ghana. The RS has similar properties albeit lower concentrations. Its Na and EC are, however, lower. It could therefore be used in most acid soils in Ghana to minimize P sorption by increasing pH.

According to Streubel (2011), most of the N is lost during pyrolysis as temperature increases from 350 to 600 ^oC. This is because as pyrolysis temperature increases, the N forms pyridine-like complexes that reduce its availability (Bagreev *et al.*, 2001). Decrease in N concentration can also

be attributed to volatilization during heating and with some of the N–containing structures in the biochar (e.g., amino acids, amines, amino sugars) condensing into recalcitrant forms and therefore may be unavailable for plant use (Cao and Harris, 2010). It is therefore a matter of consequence that all the biochar samples have low total N (< 4 g/kg) contents. The relatively higher total N content in the CP which is about 1.6 times that in the RS and the SD could be due to the higher fertilization regimes of cocoa in Ghana.

Cation exchange capacity (CEC) is defined as the sum of the total exchangeable cations that a biochar can hold or adsorb (Essay, 2013) and is also a reflection of the number of negative charges created on the surface of the material. The cation exchange capacity (38.89 – 81.67 cmol/kg) of the four biochar types was higher than the anion exchange capacity (28.12 – 39.98 cmol/kg) for the same materials. High amounts of oxygen-containing functional groups (e.g. –CO[O] and –OH) on biochars were the main reason for their high CEC (Yuan and Xu, 2012). These functional groups are likely to deprotonate in solution considering the neutral to strongly alkaline pH regimes of the four biochar types. The deprotonation will then culminate in higher CEC than AEC.

Glaser *et al.* (2002) also attributed the high CEC of biochar to the formation of carboxylic and OH groups by oxidation on the edges of the aromatic backbone of biochar. This may imply that cocoa pod with its very high polyphenol contents will possess more of the OH groups accounting for the highest cation exchange capacity of 81.67 cmol/kg. The CEC is used as a measure of the soil nutrient retention capacity, and the capacity to protect groundwater from cation contamination (Essay, 2013).

The total exchangeable bases in the four biochar types were in the order of CP > RS > SD > RH and CEC corroborates the order of CEC. The high CEC of the CP which is 30.11 cmol/kg more than the RS could therefore be taken advantage of in removing hazardous heavy metals from waste

water and soil through surface adsorption and complexation or precipitation. Its added advantage of high pH could also aid the removal process by helping to precipitate the heavy metals.

The higher AECs of the CP (38.88 cmol/kg) and the RS (I37.89 cmol/kg) than the SD (28.91 cmol/kg) and the RH (28.12 cmol/kg) imply that the former two have approximately 10 cmol/kg more positive charges than the latter two. Considering the fact that the former two particularly the CP have high pH, these materials could be used to remove anions which are pollutants from waste water. The latter two could rather be used as soil amendments to minimize leaching of anionic plant nutrients.

5.2 Sorption isotherms

The sorption isotherms fitted to the Langmuir model better than the Freundlich model implying that the four biochar surfaces have a finite number of sorption sites. With the initial P concentration not exceeding 2 mM, polymerization was avoided and thus only a single molecule occupied each sorptive site and there was no interaction between the sorbed molecules. The binding sites were identical for rice husk, sawdust and rice straw with value of 0.2 L/mg and slightly lower for cocoa pod biochar with 0.18 L/mg. The lower binding energy of the cocoa pod biochar could have accounted for its lower adsorption.

The fact that by the second hour of shaking, adsorption of phosphate onto the four biochar types was between 6900 mg/kg and 6952 mg/kg with maximum adsorption after six hours increasing by a paltry 105 mg/kg which did not show any significant difference at 5% is an indication that adsorption of P on the biochars was rapid within the first two hours of shaking. Adsorption onto an adsorbent from the aqueous phase involves three steps:

i. the transport of the adsorbate from the bulk phase to the exterior surface of the adsorbent (film diffusion),

ii. the transport into the adsorbent by either pore diffusion and/or surface diffusion (intraparticular diffusion) and

iii. the adsorption on the surface of the adsorbent which are often dependent on contact time (Kolodyn'ska *et al.*, 2012).

This means all the three processes viz film diffusion, intra-particular diffusion and adsorption were working concurrently to adsorb P onto the surface of the four biochar types and explains why within two hours, approximately 95% of the maximum adsorption had been attained (Kolodyn'ska *et al.*, 2012). This result is in conformity with a study by Zhang *et al.* (2013) who revealed that the adsorption of phosphate on biochar showed rapid kinetics and reached equilibrium within 1 hour. Adsorption capacity and removal efficiency significantly increased during the initial adsorption stage and then continue to increase at a relatively slow speed with contact time until a state of equilibrium (Mostafapour *et al.*, 2013). According to Mostafapour *et al.*, 2013, adsorbate is adsorbed easily on macropores at surfaces of the adsorbent whilst micropores surfaces adsorb more slowly due to diffusion. This may suggest that macropores surface adsorption played a significant role in the adsorption process of these four biochar types. The higher P maxima for the RH and SD may be due to a relatively larger macropore surfaces.

After the first two hours, a further increase in contact time had an insignificant effect on the amount of adsorption. This phenomenon is attributed to the fact that a large number of vacant surface sites available for adsorption at the initial stage had been saturated by the second hour, and after which the remaining adsorption was slower due to repulsive forces between the solute molecules on the solid and bulk phases (Cengiz and Cavas, 2008; Gulnaz, 2011, Mostafapour *et al.*, 2013).

The fact that at lower P concentrations there were generally no significant increases in adsorption when pH is increased from 2.7 to 7.6 but at similar pH increase, more than 1000 mg/kg P was adsorbed at higher initial P concentrations shows that initial high P concentration increases P adsorption.

The P sorption maxima for the rice husk and saw dust biochar types being about 1000 mg/kg higher than those for the CP and RS could be due to the differences in the inherent pH of the samples. Though the AEC of the CP and RS are higher than their RH and SD counterparts, the former two biochar types have higher CEC. With their strongly alkaline pH and higher CEC, the CP and RH are likely to repel more of the anionic P from their surfaces with a resultant decrease in adsorption. The lower P maxima for the CP and RS could also be due to their relatively high inherent available and total P. A higher total and available P could reduce the potential for P adsorption (Zhang *et al.*, 2013).

5.2.1 Effect of pH on adsorption

The isotherms indicated that with increasing equilibrium P concentrations, amount of P adsorbed increased. In addition, increasing equilibrium pH above the pH for maximum adsorption led to decrease in adsorption onto the various biochars. Low adsorption was observed at equilibrium pH between 2.2 and 2.8 for rice husk, sawdust and rice straw biochar. Low adsorption was also observed above equilibrium pH 7.2 for all the biochar types. Maximum adsorption onto the RH and SD biochars occurred between equilibrium pH 5.7 to 6.2 which is consistent with the findings of Yao *et al.* (2011b) and Zeng *et al.*, (2013) on other biochar types. Maximum adsorption was, however between equilibrium pH 6.7 and 7.2 for the CP and RS.

The fact that statistically similar maximum adsorption for the RH and SD occurred between equilibrium pH 5.7 and 6.2 (slightly acid) and this level of adsorption was statistically higher than

the maximum P adsorption for the CP and RS which occurred at relatively higher pHs of between 6.7 and 7.2 (neutral) suggests that pH plays an important role in P adsorption onto these biochar types. The higher pH of the RS and CS may have contributed, in part, to their lower maximum P adsorption. This trend is corroborated by the negative correlation coefficient values of between 0.85* and 0.96* when amount of P adsorbed at the various initial concentrations is regressed on equilibrium pH for CP. The fact that the correlations are negative for the CP indicates that beyond an optimum equilibrium pH of between 5.7 and 6.2, adsorption decreases. In a similar study, Zhang *et al.* (2013) found pH for maximum adsorption of P around 5.0 and Yao *et al.* (2011b) also found pH for maximum adsorption of P to be around 5.2 for other biochar types. Thus optimum pH for maximum P adsorption depends on the biochar type. The coefficient of determination for the CP was between 0.92 and 0.98 for the various initial P concentrations showing that between 92% and 98% of P adsorbed is explained by pH.

5.3 Change in pH and Ca and Mg released

A release of Ca and Mg into solution was observed at all pH for all the four samples. The amount of Ca released into solution for the sawdust biochar indicated a significant positive correlation with P adsorbed suggesting possible surface Ca precipitation of P on the sawdust biochar. Yao *et al.* (2011b) explained that when Ca is released from the biochar as free ions into solution, it may remove phosphate through precipitation.

Magnesium released into solution showed significant positive correlation with P adsorbed onto the rice husk and sawdust biochars. This implies that possible surface Mg precipitation of P could also be a mechanism of phosphate removal on the sawdust and rice hush biochars as noted by Zeng *et al.* (2013) and Yao *et al.* (2011b).

5.4 Mechanisms of adsorption

Different mechanisms will be proposed as being in part responsible for the adsorption of P on the various biochar types. Sawdust biochar showed significant correlation between the P adsorbed and Ca released into solution indicating possible Ca precipitation as a mechanism of P removal. Optimum P adsorption on the saw dust biochar type occurred at equilibrium pH 6.2. At this pH about 95% of P exists as $H_2PO_4^-$ with only about 5% existing as HPO_4^{2-} (Lindsay, 1979). Precipitation reactions at pH 6.2 may thus occur as:

$$Ca^{2+} + H_2PO_4^- \rightarrow Ca(H_2PO4)_2 \quad \textbf{(Eqn 5.1)}$$

$$Ca^{2+} + H_2PO_4^{2-} \rightarrow CaHPO_4 \quad \textbf{(Eqn 5.2)}$$

A similar reaction is proposed for Mg that was released from the RH and the SD.

$$Mg^{2+} + H_2PO_4^- \rightarrow Mg(H_2PO_4)_2 \quad \textbf{(Eqn 5.3)}$$

$$Mg^{2+} + H_2PO_4^{2-} \rightarrow MgHPO_4 \quad \textbf{(Eqn 5.4)}$$

In Eqn 5.1 and 5.3, the products are soluble and hence may be the likely surface precipitation reactions.

Magnesium oxide (MgO) present on the surfaces of cocoa pod biochar, rice straw and sawdust biochar may have removed P through electrostatic interaction and or ligand exchange. When in solution the MgO is hydroxylated. The point of zero charge (PZC) of MgO is very high near pH 12 (Kosmulski, 2009; Yao *et al.*, 2011b). The pH at which maximum adsorption occurred for the CP, RS and SD is between 6.2 and 7.2. These equilibrium pHs are between 4.8 to 5.8 pH units below the PZC. The hydroxylated surface of the MgO can then become protonated. At the pH

between 6.2 and 7.2, both H_2PO_4- and HPO_4^{2-} will exist in solution since pK2 of orthophosphoric acid is 7.2 (Lindsay, 1979). Adsorption of P on the protonated surface can then take place as:

$MgO\text{-}OH_2^+ + H_2PO_4^- \rightarrow MgO\text{-}OH_2^+ H_2PO_4^-$ (electrostatic interaction) --- (Eqn 5.5)

$MgO\text{-}OH_2^+ + H_2PO_4^- \rightarrow Mg\text{-}O\text{-}H_2PO4 + H_2O$ (Ligand exchange) ------ (Eqn 5.6)

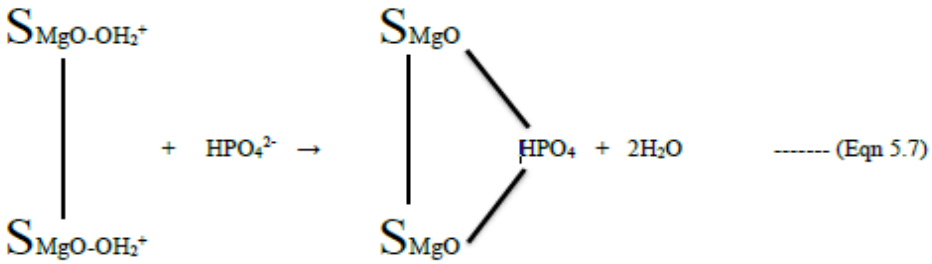

Equation 5.5 is an electrostatic one in which the orthophosphate ion is held loosely and can be exchanged by other anions into solution. The P held in this form could then be made available for plant uptake. Equation 5.6 is a mononuclear reaction involving ligand exchange where the $H_2PO_4^-$ replaces the OH_2^+ to release water into solution. Equation 5.7 is binuclear one where two of the mineral surfaces are involved. Two OH_2^+ are coordinated to the HPO_4^- releasing two moles of water into solution. The P then becomes part of the mineral structure and is not available for plant uptake.

Brucite ($Mg[OH]_2$) as a mineral was identified only in the rice husk. Its mechanism of P adsorption may therefore be different. At the optimum pH of 5.7 for maximum P adsorption, the brucite mineral could also be protonated to react with the $H_2PO_4^-$ mainly present in solution as:.

$$S_{Mg\text{-}OH} + H^+ \rightarrow S_{Mg\text{-}OH_2^+} \quad \text{--------(Eqn 5.9)}$$

$$S_{Mg\text{-}OH_2^+} + H_2PO_4^- \rightarrow S_{Mg\text{-}OH_2^+ H_2PO_4^-} \text{ (Electrostatic interaction)} \quad \text{--- (Eqn 5. 10)}$$

$$S_{Mg\text{-}OH_2^+} + H_2PO_4^- \rightarrow S_{Mg\text{-}H_2PO_4} + H2O \text{ (Ligand exchange)} \quad \text{---------- (Eqn 5. 11)}$$

From the change in pH values in adsorption, there was generally no change in pH except in the SD and RS where there was decrease in pH at the maximum adsorption. This decrease in pH connotes proton release as a result of adsorption which for now is inexplicable. The no change in pH observed on the cocoa pod and rice husk biochar types could be a confirmation of the proposed reactions where water is released into solution after adsorption.

CHAPTER SIX

CONCLUSIONS AND RECOMMENDATION

6.1 Conclusions

The study revealed that cocoa pod, rice husk, sawdust and rice straw charred at 450 ^{o}C produced biochar types with varying ash contents, chemical and mineralogical composition. The rice husk and the cocoa pod biochar types had the highest ash contents at charring temperature of 450 ^{o}C suggesting that they are more prone to combustion.

The cocoa and rice straw biochar have strongly alkaline pH with large amounts of $KHCO_3$ in the CP and $CaCO_3$ in the RS suggesting that these two biochar types could be exploited for use as cheap liming materials.

The study has shown that six hours of shaking is optimum for adsorption of P onto biochar and that optimum equilibrium pH for maximum adsorption of P for biochar is between 5.7 and 7.2. Maximum P sorption capacities for the sawdust and rice husk biochar types were estimated to be 7300 mg/kg with binding energies of 0.2 L/mg. The maximum P sorption capacity for the rice straw biochar was estimated to be 6300 mg/kg with a binding energy of 0.2 L/mg. The cocoa pod biochar had the least P sorption capacity of 6200 mg/kg and a binding energy of 0.18 L/mg due to in part, its strongly alkaline pH of 10.4

Phosphate adsorption mechanism varied with biochar type. Surface precipitation by Ca and Mg was an important mechanism of P adsorption onto the sawdust biochar with Mg precipitation also proposed as an important mechanism of P adsorption onto the rice husk biochar. Both electrostatic attraction and ligand exchange reactions by periclase (MgO) with P was the main mechanisms of adsorption on cocoa pod, rice straw and sawdust biochar types. Electrostatic attraction and ligand

exchange of orthophosphate ion with brucite was proposed as the main mechanism of adsorption on the rice husk biochar.

6.2 Recommendations

In order to make the findings of this research useful, field application of the P enriched biochar to study the bioavailability of the adsorbed nutrients, rate of nutrient release upon soil amendment vis-a-vis productivity of the soil should be studied.

Post adsorption mineralogical studies including spectroscopy (NMR, FTIR) and Scanning Electron Microscopy (SEM) and surface properties (surface acidity) studies be carried out to fully elucidate the mechanism of adsorption of P on the different biochar types.

REFERENCES

Agyei, N.M., Strydom, C.A., and Potgieter, J.H. 2000. An investigation of phosphate ion adsorption from aqueous solution by fly ash and slag. Cement Concrete. Res. 30: 823.

Agyei, N.M., Strydom, C.A., and Potgieter, J.H. 2002. The removal of phosphate ions from aqueous solution by fly ash, slag, ordinary Portland cement and related blends. Cement Concrete Res. 32:1889-1897.

Amonette, J., and S. Joseph, S. 2009. Characteristics of biochar: Micro-chemical properties. p. 33¬52. In J. Lehmann and S. Joseph (eds.) Biochar for environmental management: Science and technology. Earthscan, London.

Anbia, M., and Hariri, S.A. 2010. Removal of methylene blue from aqueous solution using nanoporous SBA-3. Desalination 26(1-2): 61-66.

Anderson, J.M., Ingram, J.S.I. (Eds.) 1993. Tropical soil biology and fertility: a handbook of methods. CAB International, Wallingford, UK.

Antal Jr, M.J. and Gronli, M., 2003.The art, science, and technology of charcoal production. Industrial and Engineering Chemistry Research 42(8): 1619-1640.

Antwi-Bosiako, R. 2012. Physico-chemical properties of biochar produced from three feedstocks. A B.Sc Dissertation, Department of Soil Science, College of Agric. And Consumer Sciences. University of Ghana, Legon. 42pp.

Arias, C., Bubba, M., and Brix, H. 2001. Phosphorus removal by sands for use as media in subsurface flow constructed reed beds. Water Res. 35(5):1159-1168.

Bagreev, A., Bandoz, T.J., and Locke, D.C. 2001. Pore structure and surface chemistry of adsorbents obtained by pyrolysis of sewage sludge-derived fertilizer. Carbon. 39: 1971-1977.

Banu, R.J., Dou, K.U., and Yeom, I.T. 2008. Phosphorus removal in low alkalinity secondary effluent using alum. Int. J. Environ. Sci. Tech. 5: 93-98.

Bellier, N., Chazarenc, F., and Y. Comeau. 2006. Phosphorus removal from wastewater by mineral apatite. Water Res. 40: 2965-2971.

Bhargava, D.S., and Sheldarkar, S.B., 1993. Use of Tnsac in phosphate adsorption studies and relationships - isotherm relationships and utility in the field. Water Res. 27(2): 325¬335.

Brown, R. 2009. Biochar: Production technology. pp. 127-146. In J. Lehmann and S. Joseph (eds.). Biochar for environmental management: Science and technology. Earthscan, London (2009).

Brownsort P.A. 2009. Review of scope, control and variability. UKBRC working paper 5: 2. www.geos.ed.ac.uk/sccs/biochar/documents/WP5.pdf.

Cao, X. and Harris, W. 2010. Properties of dairy-manure-derived biochar pertinent to its potential use in remediation, Bioresource Techol. 101: 5222-5228.

Cengiz, S., and Cavas, L. 2008. Removal of methylene blue by invasive marine seaweed: Bioresource Technology 99(7): 2357-2363.

Chan K.Y., and Xu, Z. 2009. Biochar: nutrient properties and their enhancement. In Lehmann J, Joseph S, editiors. Biochar for environmental management, science and technology. London, UK: Earthscan; 2009. 67-84.

Chen, B.L., Zhou, D.D., and Zhu, L.Z. 2007. Transitional adsorption and partition of nonpolar and polar aromatic contaminants by biochars of pine needles with different pyrolytic temperatures, Environ. Sci. Technol. 42: 5137-5143.

Chen, B.L., Zhou, D.D., and Zhu, L.Z. 2008. Transitional adsorption and partition of nonpolar and polar aromatic contaminants by biochars of pine needles with different pyrolytic temperatures, Environ. Sci. Technol. 42: 5137-5143.

Chun, Y., Sheng, G.Y., Chiou, C.T., and Xing, B.S. 2004. Compositions and sorptive properties of crop residue-derived chars, Environ. Sci. Technol. 38: 4649-4655.

Cooney, D.O. 1999. Adsorption design for wastewater treatment. CRC Press LLC, Boca Raton.

Crutzen, P.J., and Andreae, M.O., 1990. Biomass burning in the tropics: impact on atmospheric chemistry and biogeochemical cycles. Science 250: 1669-1678.

Cucarella, V., and Renman, G. 2009. Phosphorus sorption capacity of filter materials used for on-site wastewater treatment determined in batch experiments-A Comparative Study. J. Environ. Qual. 38:381-392.

Dada, A.O., Olalekan, A.P., Olatunya, A.M. and Dada, O. 2012. Langmuir, Freundlich, Temkin and Dubinin-Radushkevich isotherms studies of equilibrium sorption of Zn2+ onto phosphoric acid modified rice husk. Journal of Applied Chemistry 3(1): 38-45.

Das, J., Patra, B.S., Baliarsingh, N., Parida, K.M., 2006. Adsorption of phosphate by layered double hydroxides in aqueous solutions. Appl. Clay Sci. 32: 252-260.

Day, D., Evans, R.J., Lee, J.W. and Reicosky, D. 2005. Economical CO_2, SOx, and NOx capture from fossil-fuel utilization with combined renewable hydrogen production and large- scale carbon sequestration. Energy 30: 2558-2579.

de-Bashan, L.E and Bashan, Y. 2004. Recent advances in removing phosphorus from wastewater and its future use as fertilizer (1997-2003). Water Research 38: 4222-4246.

Delhaize, E. and Ryan, P.R. 1995. Aluminum toxicity and tolerance in plants. Plant Physiol. 107: 315-321.

Delle, A.S. 2001. Factors affecting sorption of organic compounds in natural sorbent/water systems and sorption coefficients for selected pollutants. A Review. J. Phys. Chem. 30(1): 187-439.

Demirbas. 2004. Adsorption of lead and calcium ions in aqueous solutions onto modified lignin from alkali glycerol delignication, J. Hazard. Mater. 221-226.

Demirbas, A. 2001. Carbonisation ranking of selected biomass for charcoal, liquid and gaseous products. Energy Conversion and Management. 42: 1229-38.

Doerge. T. 1999. Soil Electrical Conductivity Mapping. Crop Insights, Vol. 9 No. 19.

Domi'guez, A., Mene'dez, J.A., Inguanzo, M., and Pi', J.J., 2006.Production of bio-fuels by high temperature pyrolysis of sewage sludge using conventional and microwave heating. Bioresour. Technol. 97 (10): 1185-1193.

Downie, A., Crosky, A., and Munroe, P. 2009. Physical properties of biochar. In: Lehmann J, Joseph S, editors. Biochar for environmental management: science and technology. London, UK: Earthscan.

Duku, M.H., Gu, S., and Hagan, E.B. 2011. Biochar production potential in Ghana - A review. Renew. Sust. Energy Rev. 15: 3539-3551.

Eduah, J.O. 2012. Removal of nitrate, phosphorus and *Escherichia coli* from simulated wastewater using modified biosand filter system. M.Phil Thesis presented to University Ghana, Department of soil science.

Essays, 2013. Factors Affecting Cation Exchange Capacity Environmental Sciences Essay.

Retrieved from http://www.ukessays.com/essays/environmental-sciences/factors- affecting-cation-exchange-capacity-environmental-sciences-essay.php?cref=1. FAO. 2011. Save and grow: A policymaker's guide to the sustainable intensification of smallholder crop production. SBN 978-92-5-106871-7: 112.

Figueira, A., Janick, J., and BeMiller, J.N. 1993. New products from Theobroma cacao: Seed pulp and pod gum. p. 475-478. In: J. Janick and J.E. Simon (eds.), New crops. Wiley, New York.

Foray, J.Jnr. (2012). Solid Waste management in Ghana. A comprehensive case for West Africa.

Africans reality group. Retrieved from: http://africanreality.over-blog.net/article- solid-waste-managment-in-ghana-a-comprehensive-case-for-west-africa- 107960790.html on 28th June, 2014.

Freundlich, H. 1926. Colloid and Capillary Chemistry. Methuen & Co. Ltd., London. 110-114.

Frimpong-Manso, J., Obodai, M., Dzomeku, M. and Apertorgbor, M.M. 2011. Influence of rice husk on biological efficiency and nutrient content of *Pleurotus ostreatus* (Jacq. ex. Fr.) Kummer. International Food Research Journal 18: 249-254.

Fu, P., Hu, S., Xiang, J., Sun, L.S., Li, P.S., Zhang, J.Y., and Sheng, C.G. 2009. Pyrolysis of maize stalk on the characterization of chars formed under different devolatilization conditions. Energy Fuels, 23(9):4605-4611. (doi:10.1021/ef900268y).

Gao, J., and Pedersen, J.A. 2005. Adsorption of sulfonamide antimicrobial agents to clay minerals. Environ Sci Technol 39: 9509-9516.

Gaskin, J. W., Steiner, C., Harris, K., Das, K. C. and Bibens, B. 2008. Effect of low-temperature pyrolysis conditions on biochar for agricultural use. T. ASABE. 51: 2061-2069.

Gaunt, J., and Lehmann, J. 2008. Energy balance and emissions associated with biochar Sequestration and pyrolysis bioenergy production. Environmental Science & Technology, 42: 4152-8.

Gerritse, R.G. 1993. Prediction of travel times of phosphate in soils at a disposal site for wastewater. Water Res. 27(2): 263-267. (doi:10.1016/0043-1354(93)90084-U).

Glaser, B., Lehmann, J., and Zech, W. 2002. Ameliorating physical and chemical properties of highly weathered soils in the tropics with charcoal: a review. Biology and Fertility of Soils 35: 219-230.

Goh, K.H., Lim, T.T., and Dong, Z. 2008. Application of layered double hydroxides for removal of oxyanions: A review. Water Res. 42: 1343-1368.

Granatstein, D., Kruger, C., Collins, H.P., Garcia-Perez, M, and Yoder, J. 2009. Use of biochar from the pyrolysis of waste organic material as a soil amendment. Center for Sustaining Agric. Nat. Res. Washington State University, Wenatchee, WA.WSDA Interagency Agreement. C0800248. (http://www.ecy.wa.gov/pubs/0907062.pdf).

Grassi, M., Kaykioglu, G., Vincenzo Belgiorno, V., and Lofrano, G. 2012. Removal of emerging contaminants from water and wastewater by adsorption process. Green Chemistry for Sustainability. 15: 33.

Gulnaz, O., Sahmurova, A., and Kama, S. 2011. Removal of reactive red 198 from aqueous solution by *Potamogeton crispus*. Chemical Engineering Journal 174(2-3): 579-585.

Han, X., Cheng-Feng Liang, C., Ting-qiang Li, Kai Wang, K., Hua-gang Huang, H., and Yang, X. 2013. Simultaneous removal of cadmium and sulfamethoxazole from aqueous solution by rice straw biochar. J. Zhejiang Univ. Sci. B. 14(7): 640-649.

Harvey, O.R., Herbert, B.E., Rhue, R.D., and Kuo, L.J. 2011. Metal interactions at the biochar-water interface: energetics and structure-sorption relationships elucidated by flow adsorption microcalorimetry. Environ. Sci. Technol. 45(13):5550-5556.

Hossain, M.K., Strezov, V., Chan, K.Y., and Nelson, P.F. 2010. Agronomic properties of wastewater sludge biochar and bioavailability of metals in production of cherry tomato (Lycopersicon esculentum). Chemosphere 78 (9): 1167-1171.

Hossain, M.K., Strezov, V., Chan, K.Y., Ziolkowski, A., and Nelson, P.F. 2011. Influence of pyrolysis temperature on production and nutrient properties of wastewater sludge biochar. J. Environ. Manage. 92 (1), 223-228.

Huang, W.L., Ping, P.A., Yu, Z.Q., and Fu, H.M. 2003. Effects of organic matter heterogeneity on sorption and desorption of organic contaminants by soils and sediments. Appl. Geochem. 18: 955-972.

Hwang, I.H., Ouchi, Y., and Matsuto, T., 2007. Characteristics of leachate from pyrolysis residue of sewage sludge. Chemosphere 68 (10): 1913-1919.

International Atomic Energy Agency (IAEA). 2002. Assessment of soil phosphorus status and management of phosphaticic fertilizers to optimize crop production. Vienna, IAEA-TECDOC-1272ISSN: 1011-4289.

Kaczala, F., Marques, M., and Hogland, W. 2009. Lead and vanadium removal from a real industrial wastewater by gravitational settling/sedimentation and sorption onto *Pinus sylvestris* sawdust. Bio resource Technology 100(1): 235-243.

Kah, M. 2007. Behaviour of ionisable pesticides in soils. Doctor of Philosophy thesis submitted to University of York, Environment Department. 46-55.

Khattri, S.D., and Singh, M.K. 2009. Removal of malachite green from dye wastewater using neem sawdust by adsorption. J Hazard Mater 167: 1089-1094.

Kolodynska, D., Wnetrzak, R., Leahy, J. J., Hayes, M.H.B., Kwapin, W., and Hubicki, Z. 2012. Kinetic and adsorptive characterization of biochar in metal ions removal. Chemical Engineering Journal 197: 295-305.

Kosmulski, M. 2009. Surface Charging and Points of Zero Charge. Taylor & Francis Group, Boca Raton.

Krull, E.S., Baldock, J.A., Skjemstad, J.O., and Smernik, R.J. 2009. Characteristics of biochar: Organo-chemical properties. pp. 53-65. In J. Lehmann and S. Joseph (eds.) Biochar for environmental management: Science and technology. Earthscan, London.

Kuwagaki, H., Tamura, K. 1990. Aptitude of wood charcoal to a soil improvement and other non-fuel use. In: Mitigation and adaptation strategies for global change. Laird, D. A., Brown, R.C., Amonette, J.E., and Lehmann, J. 2009. Review of the pyrolysis platform for coproducing bio-oil and biochar. Biofuels, Bioprod. Bioref. 3: 547-562.

Langmuir, I. 1918. The Adsorption of Gases on Plane Surfaces of Glass, Mica and Platinum. J. Am. Chem. Soc. 40: 1361.

Lehmann, .J. and Joseph, S. 2009. Biochar for environmental management: science and technology. Earthscan, Sterling, VA. 1-12.

Lehmann, J. 2007. A handful of carbon. Nature 447: 143-144.

Lehmann, J., Gaunt, J., and Rondon, M. 2006. Bio-char sequestration in terrestrial ecosystems - A review. Mitigation and Adaptation Strategies for Global Change. 11: 395-419.

Li, Q., Xu, XT. Cui, H., Pang, J., Wei, Z.B., Sun, Z., and J. Zhai, J. 2012. Comparison of two adsorbents for the removal of pentavalent arsenic from aqueous solutions. Journal of Environmental Management 98: 98-106.

Liang, B., Lehmann, J., Solomon, D., Kinyangi, J., Grossman, J., O'Neill, B., Skjemstad, J.O., Thies, J., Luizao, F. J., Petersen, J. and Neves, E.G. 2006. Black carbon increases cation exchange capacity in soils. Soil Science Society of America Journal 70: 1719¬1730.

Lindsay, W.L. 1979. Chemical equilibria in soils. John Wiley and Sons, Inc., United State of America.

Liu, P., Kendelewicz, T., Brown, E.G., Nelson, E.J., and Chambers, S.A. 1998. Reaction of water vapor with a-Al_2O_3(0001) and a -Fe_2O_3(0001) surfaces: Synchrotron X-ray photoemission studies and thermodynamic calculations. Surface Science 417: 53-65.

Lu S.G., Bai, S.Q., Zhu, L., and Shan, H.D. 2009. Removal mechanism of phosphate from aqueous solutions by fly ash. J. Haz. Mat. 161: 95-101.

Lu, H., Zhang, W., Yang, Y., Huang, X., Wanga, S. and Qiu. R. 2011. Relative distribution of Pb2+ sorption mechanisms by sludge-derived biochar. Water research 46: 854 -862.

Luo, L., Lou, L P., Cui, X.Y., Wu, B.B., Hou, J., Xun, B., Xu, X.H., and Chen, Y.X. 2011. Sorption and desorption of pentachlorophenol to black carbon of three different origins. J. Hazard. Mater 185: 639-646.

Manning, B.A., and Goldberg, S. 1996. Modeling competitive adsorption of arsenate wit phosphate and molybdate on oxide minerals, Soil Sci. Soc. Am. J. 60: 121-131.

McGechan, M.B., and D.R. Lewis. 2002. Sorption of phosphorus by soil: Part 1. Principles, equations, and models. Biosyst. Eng. 82:1-24.

Meidl, J.A. 1997. Responding to changing conditions: how powdered activated carbon systems can provide the operational flexibility necessary to treat contaminated groundwater and industrial waste. Carbon. 35: 1207-1216.

Mesa, A.C., and Kurt, S. 2011. Impacts of biochar (black carbon) additions on the sorption and efficacy of herbicides. Herbicides and Environment 15:316-332.

Mohan, S., and Karthikeyan, J. 1997. Removal of lignin and tannin color from aqueous solution by adsorption on to activated carbon solution by adsorption on to activated charcoal'', Environ. Pollut. 97.183-187.

Moreno-Castilla, C. 2004. Adsorption of organic molecules from aqueous solutions on carbon materials. Carbon 42: 83-94.

Mostafapour, F.K., Bazrafshan, J., Farzadkia, M., and Amini, S. 2013. Arsenic removal from aqueous solutions by *salvadora persica* stem ash. Journal of Chemistry 740847: 8.

Murphy, J and Riley, J.P. 1962. A modified single solution method for the determination of phosphate in natural water. Analytical Chemistry Acta 27:31-36.

Naeem, A., Westerhoff, P., and Mustafa, S. 2007. Vanadium removal by metal hydroxide adsorbents. Water Res 41: 1596-1602.

Namasivayam, C., and Sangeetha, D. 2004. Equilibrium and kinetic studies of adsorption of phosphate onto $ZnCl_2$ activated coir pith carbon. J. Colloid Interface Sci. 280 (2):359- 365.

Nartey, E., Dowuona, G.N., Ahenkorah, Y., and Mermut, A.R. 1997. Variability in the properties of soil on two topsequences in northern Ghana. Ghana Journal of Agriculture Science 30:115-126.

Nartey, E., Matsue, N. and Henmi, T. 2000. Adsorptive mechanism of orthosilic acid on nano-ball allophane. Clay Science 11(2): 152-135.

Nartey, E., Matsue, N. and Henmi, T. 2001. Charge characteristics modification mechanism of nano-ball allophane upon orthosilicic acid adsorption. Clay Science 11: 465 – 477.

Novak, J., Busscher, W., Watts, D., Laird, M., Ahmedna, and M. Niandou. 2009. Short-term CO2 mineralization after additions of biochar and switch grass to a Typic Kandiudult. Geoderma 154: 281-288.

Ogawa, M., Okimori, Y., and Takashi, F. 2006. Carbon sequestration by carbonisation of biomass and forestation: three case studies. Mitigation and Adaptation Strategies for Global Change 11: 421-36.

Oguz, E. 2005. Sorption of phosphate from solid/liquid interface by fly ash. Colloids and Surf. Physicochem. Engin. Aspects 262: 113-117.

Owusu-Bennoah, E., Fardeau, I.C. and Zapata, F. 2000. Evaluation of bioavailable phosphorus in some acid soils of Ghana using 32p isotopic exchange method. Ghana Journal Agriculture Science 33: 139-146.

Pandey, P.K., Choubey, S., Verma, Y., Pandey, M., and Chandrashekhar, K. 2009. Biosorptive removal of arsenic from drinking water. Bioresource Technology 100(2): 634-637.

Putra, E. K., Pranowo, R., Sunarso, J., Indraswati, N., and Ismadji, S. 2009. Performance of activated carbon and bentonite for adsorption of amoxicillin from wastewater: Mechanisms, isotherms and kinetics. Water Res 43: 2419-2430.

Qafoku, N. P. *et al.* 2004. Variable charge soils: Their mineralogy, chemistry and management. In Advances in Agronomy 84, ed. D. L. Sparks, 159-215, New York: Academic Press.

Rumhayati, B., Bisri, C., Kusumawati, H., and Yasmin, F. 2012. Phosphate and nitrate removal from drinking water sources using acrylamide-ferrihydrite gel. Indo. J. Chem. 12 (3): 287-290.

Schindler, P.W., and Stumm, W. 1987. The surface chemistry of oxides, hydroxides, and oxide minerals. In: Stumm, W. (Ed.), Aquatic surface chemistry - chemical processes at the particle-water interface. John Wiley & Sons, New York.

Shin, E.W., Han, J.S., Jang, M., Min, S.H., Park, J.K., and Rowell, R.M. 2004. Phosphate adsorption on aluminum-impregnated mesoporous silicates: surface structure and behavior of adsorbents, Environ. Sci. Technol. 38: 912-917.

Shinogi, Y., and Kanri, Y. 2003. Pyrolysis of plant, animal and human waste: physical and chemical characterization of the pyrolytic products. Bioresour. Technol. 90: 241-247.

Sohi, S., Lopez-Capel, E., Krull, E., and Bol, R. 2009. Biochar, climate change and soil: a review to guide future research. CSIRO Land and Water Science Report.

Sombroek, W. 1966. Amazon soils; a reconnaissance of the soils Brazilian Amazon region. Centre for Agricultural Publications and Documentation, PUDOC, Wageningen.

Sposito, G. 2008. The Chemistry of Soils, 2nd ed. New York, NY: Oxford University Press.

Steiner, C., Teixeira, W.G., Lehmann, J., Nehls, T., Vasconcelos de Macedo, J. L., Blum, W.E.H. and Zech, W. 2007. Long term effects of manure, charcoal and mineral fertilization on crop production and fertility on a highly weathered Central Amazonian upland soil. Plant Soil. 291: 275-290.

Strahm, B.D., and Harrison, R.B. 2006. Nitrate sorption in a variable-charge forest soil of the Pacific Northwest. Soil Sci. 171 (4): 313-321.

Streubel, J.D. 2011. Biochar: Its characterization and utility for recovering phosphorus from anaerobic digested dairy effluent. Doctor of Philosophy dissertation submitted to Washington State University, Department of Crops and Soils. pp34.

Stumm, W. and Schindler, P.W. 1987. The surface chemistry of oxides, hydroxides, and oxide minerals, in: W. Stumm (Ed.), Aquatic Surface Chemistry—Chemical Processes at the Particle-Water Interface, John Wiley & Sons, New York.

Stumm, W., and Morgan, J.J. 1996. Aquatic chemistry: Chemical equilibria and rates in natural waters, 3rd ed. Wiley-Interscience, New York.

Sustainable Tree Crops Program (STCP). 2007. Farm safety interventions in the cocoa sector. International Institute of Tropical Agriculture, Issue .07.

Tan, H.K. 2011. Principles of soil chemistry (Fourth edition). Taylor and Francis Group, Broken Sound Parkway, NW, Boca Ratoion. 175-188.

Tang, J., Zhu, W., Kookana, R. and Katayama, A. 2013. Characteristics of biochar and its application in remediation of contaminated soil. J. Biosci. Bioeng., 20(20): 1-7.

Thompson, A. and Goyne, K.W. (2012) Introduction to the sorption of chemical constituents in soils. Nature Education Knowledge 4(4):1-7.

Uchimiya, M., Wartelle, L.H., Lima, I.M., Klasson, K.T. 2010. Sorption of deisopropylatrazine on broiler litter biochars. J. Agric. Food Chem. 58: 12350-12356.

Ueno, M., Kawamitsu, Y., Komiya, Y., Sun, L. 2007. Carbonisation and gasification of bagasse for effective utilisation of sugarcane biomass. International Sugar Journal 110: 22-26.

United Nations Industrial Development Organization. 2009. Waste stock exchange management system in Ghana. Third Progress Report. GP/RAF/04/004: 1-19.

USDA Foreign Agriculture Service. 2012. Cocoa Report Annual, Ghana.

Verheijen, F., Jeffery, S., Bastos, A.C., van der Velde M., Diafas I. 2010. Biochar application to soils: a critical scientific review of effects on soil properties, processes and functions. European Commission; (http://eusoils.jrc.ec.europa.eu/esdbarchive/eusoils docs/other/EUR24099.pdf).

Voudrias, E., Fytianos, F., and Bozani, E. 2002. Sorption description isotherms of dyes from aqueous solutions and wastewaters with different sorbent materials. Global Nest, The Int. J. 4(1): 75-83.

Walkley, A., and Black, I.A. 1934. An examination of the dehtjareff method for determining soils organic matter, and a proposed modification of the chromic acid titration method. Soil Science. 37: 29-38.

Webb, P.A. 2003. Introduction to Chemical Adsorption Analytical Techniques and their Applications to Catalysis. MIC Technical Publications: 1-8.

Weber, W.J., McGinley, P.M., and Katz, L. E. 1991. Sorption phenomenon in subsurface systems: concept and models and effect on contaminant fate and transport. Water Res. 25: 499 528.

Woolf, D. 2008. Biochar as a soil amendment - a review of the environmental implications.

Swansea University. International Rice Research Institute, Black Soil, Green Rice, Rice Today; April-June 2007.

Yao, Y., Gao, B., Inyang, M., Zimmerman, A. R,. Cao, X., Pullammanappallil, P., and Yang, L. 2011a. Biochar derived from anaerobically digested sugar beet tailings: Characterization and phosphate removal potential, Bioresour. Technol. doi:10.1016/j.biortech.2011.1003.1006.

Yao, Y., Gao, B., Inyang, M., Zimmerman, A.R., Cao, X., Pullammanappallil, P., Yang, L., 2011b. Removal of phosphate from aqueous solution by biochar derived from anaerobically digested sugar beet tailings. J. Hazard. Mater. 190, 501–507.

Yao, Y., Gao, B., Zhang, M., Inyang, and M., Zimmerman, A. 2012. Effect of biochar amendment on sorption and leaching of nitrate, ammonium, and phosphate in a sandy soil. Chemosphere 89: 1467-1471.

Yao, Y., Bin, Gao, B., Chen, J., Zhang, M., Inyang, M., Li, Y., Ashok Alva, A., and Yang, L. 2013. Engineered carbon (biochar) prepared by direct pyrolysis of Mg-accumulated tomato tissues: Characterization and phosphate removal potential. Bioresource Technology 138: 8-13.

Yuan, J., and Xu, R. 2012. Effects of biochars generated from crop residues on chemical properties of acid soils from tropical and subtropical China. Soil Research 50(7): 570-578.

Zeng, Z., Song-da, Z., Ting-qiang, L., Fen-liang, Z., Zhen-li, H., He-ping, Z., Xiao-e, Y., Hai-long, W., Jing, Z., and Mohammad, T.R. 2013. Sorption of ammonium and phosphate from aqueous solution by biochar derived from phytoremediation plants. Biomed and Biotechnol, 14(12): 1152-1161.

Zhang, H., Huang, C. H. 2007. Adsorption and oxidation of fluoroquinolone antibacterial agents and structurally related amines with goethite. Chemosphere l 66: 1502-1512.

Zhang, M., Gao, B., Yao, Y., and Inyang, M. 2013. Phosphate removal ability of biochar/MgAl-LDH ultra-fine composites prepared by liquid-phase deposition. Chemosphere 92: 1042-1047.

Zhang, Q., Yang, Z., Wu, W. 2008. Role of crop residue management in sustainable agricultural development in the North China Plain. Journal of Sustainable Agriculture 32(1): 137¬48. (http://www.informaworld.com).

Zheng, Z., Song-da, Z., Ting-qiang, L., Fen-liang, Z., Zhen-li, H., He-ping, Z., Xiao-e, Y., Hai-long, W., Jing, Z., and Mohammad, T.R. 2013. Sorption of ammonium and phosphate from aqueous solution by biochar derived from phytoremediation plants. Biomed and Biotechnol, 14(12): 1152-1161.